BRAIN
ORIGINAL ARTICLE

Lymphotoxin-alpha expression in the meninges causes lymphoid tissue formation and neurodegeneration

Rachel E. James Bates,[1,†] Eleanor Browne,[1,†] Renee Schalks,[1] Heather Jacobs,[1] Li Tan,[1] Puja Parekh,[1] Roberta Magliozzi,[1,2] Massimiliano Calabrese,[2] Nicholas D. Mazarakis[1] and Richard Reynolds[1,3]

[†]These authors contributed equally to this work.

Organized meningeal immune cell infiltrates are suggested to play an important role in cortical grey matter pathology in the multiple sclerosis brain, but the mechanisms involved are as yet unresolved. Lymphotoxin-alpha plays a key role in lymphoid organ development and cellular cytotoxicity in the immune system and its expression is increased in the CSF of naïve and progressive multiple sclerosis patients and post-mortem meningeal tissue. Here we show that persistently increased levels of lymphotoxin-alpha in the cerebral meninges can give rise to lymphoid-like structures and underlying multiple sclerosis-like cortical pathology. Stereotaxic injections of recombinant lymphotoxin-alpha into the rat meninges led to acute meningeal inflammation and subpial demyelination that resolved after 28 days, with demyelination being dependent on prior subclinical immunization with myelin oligodendrocyte glycoprotein. Injection of a lymphotoxin-alpha lentiviral vector into the cortical meningeal space, to produce chronic localized overexpression of the cytokine, induced extensive lymphoid-like immune cell aggregates, maintained over 3 months, including T-cell rich zones containing podoplanin + fibroblastic reticular stromal cells and B-cell rich zones with a network of follicular dendritic cells, together with expression of lymphoid chemokines and their receptors. Extensive microglial and astroglial activation, subpial demyelination and marked neuronal loss occurred in the underlying cortical parenchyma. Whereas subpial demyelination was partially dependent on previous myelin oligo-dendrocyte glycoprotein immunization, the neuronal loss was present irrespective of immunization. Conditioned medium from LTα treated microglia was able to induce a reactive phenotype in astrocytes. Our results show that chronic lymphotoxin-alpha overexpression alone is sufficient to induce formation of meningeal lymphoid-like structures and subsequent neurodegeneration, similar to that seen in the progressive multiple sclerosis brain.

1 Division of Neuroscience, Department of Brain Sciences, Imperial College London, Hammersmith Hospital Campus, London, UK
2 Neurology Section, Department of Neurological and Movement Sciences, University of Verona, Verona 37134, Italy
3 Centre for Molecular Neuropathology, Lee Kong Chian School of Medicine, Nanyang Technological University, Singapore

Correspondence to: Professor Richard Reynolds
Department of Brain Sciences, Imperial College Faculty of Medicine
Hammersmith Hospital Campus, Burlington Danes Building
Du Cane Road, London W12 0NN, UK
E-mail: r.reynolds@imperial.ac.uk

Introduction

The progressive stages of multiple sclerosis are characterized by an increasing burden of grey matter (GM) pathology that is suggested to play a major role in the irreversible accumulation of sensory, cognitive and motor symptoms.[1–5] Accumulating axon and neuronal loss that are stimulated by an ongoing compartmentalized inflammation are now widely accepted to be one of the main pathological drivers of clinical progression.[6–8] Recent studies on human post-mortem tissues have suggested that chronic inflammation in the leptomeninges may be one of the main pathogenetic mechanisms underlying the development of cortical pathology.[9–12] The presence of leptomeningeal inflammation and the development of tertiary lymphoid-like structures (TLS) in the subarachnoid space (SAS)[9,13] correlate with a gradient of neuronal loss in the cerebral cortical GM that is associated with a shorter time to milestones of clinical progression, including a shorter time to wheelchair use, shorter disease duration and younger age at death.[6,10] These TLS are characterized by discrete aggregates of B and T cells, plasma cells, antigen-presenting cells and a network of follicular dendritic cells,[9,13,14] display varying degrees of organization and may serve as sites for autoantigen presentation and intrathecal antibody production, both of which are important in driving inflammation in chronic multiple sclerosis.[15,16] Meningeal inflammation is seen from the very early stages of multiple sclerosis[17,18] and in multiple CNS locations,[6,19,20] but the molecular and cellular mechanisms involved in the formation and maintenance of these immune cell aggregates remain unclear.

The presence of compartmentalized inflammation in the meninges and the underlying gradient of pathology in the cortical GM has given rise to the hypothesis that proinflammatory cytokines and other cytotoxic molecules in the CSF may diffuse into the underlying cortex and directly or indirectly initiate cellular damage.[8,21–23] This also raises the possibility that the same molecule(s) that are involved in stimulating the development of lymphoid tissues could also be responsible for aspects of the cortical cell damage. Analysis of the composition of post-mortem and patient CSF of multiple sclerosis cases with increased cortical pathology[12,24] has revealed the elevated presence of proinflammatory cytokines [e.g. IFNγ, tumour necrosis factor (TNF), IL2, IL6], molecules related to B-cell activation (e.g. BAFF, APRIL, LIGHT, IL10) and lymphoid neogenesis (e.g. LTα, CXCL13, CXCL10). Of these molecules, lymphotoxin-α (LTα) is known to have a role in cellular cytotoxicity, lymphoid neogenesis and TLS formation,[25–27] but its involvement in the pathogenesis of multiple sclerosis has been little studied. Lymphotoxin-α can form a soluble homotrimer that binds to TNF receptors 1 and 2 (TNFR1/TNFR2) and can also form heterotrimers together with LTβ, as either LTα2β1 or LTα1β2, which remain tethered in the cell membrane and bind to the LTβ receptor (LTβR). LTα has been previously suggested to play a role in the pathogenesis of multiple sclerosis due to its ability to potently induce apoptosis of oligodendrocytes *in vitro*,[28] and its expression by CD3+ lymphocytes and microglia at the border of acute and chronic active multiple sclerosis lesions.[29–31] Increased LTα mRNA expression was observed in peripheral blood lymphocytes before relapse in relapsing remitting multiple sclerosis (RRMS), and expression was strongly upregulated by stimulation with myelin basic protein (MBP) *in vitro*, suggesting that LTα may play a role in the exacerbation of multiple sclerosis.[32,33] Increased LTα expression has also been demonstrated in peripheral blood B cells[34] and increased release by CD8+ T cells noted in SPMS patients.[35]

LTα is known to play a key role in lymphoid tissue organogenesis and maintenance.[26] Mice that are deficient in LTα have significant defects in the development of lymphoid organs, specifically lacking secondary lymphoid organs, including lymph nodes and Peyer's patches,[36] and are resistant to experimental autoimmune encephalomyelitis (EAE) induced in C57Bl6 mice by immunization with myelin oligodendrocyte glycoprotein (MOG) peptide 35–55.[37] In contrast, ectopic transgenic expression of LTα driven by the rat insulin promotor caused chronic inflammation and TLS formation in the kidney and pancreas.[25] While LTα has been shown to be a key player in formation of TLS in the lung during influenza and in synovial tissue in rheumatoid arthritis,[38] the role of LTα in chronic leptomeningeal inflammation and CNS TLS formation has yet to be examined.

Meningeal inflammation accompanied by various stages of TLS formation has been reported in several animal models of multiple sclerosis, including the relapsing remitting form of EAE (rrEAE) in the SJL/J mouse immunized with PLP peptide,[39,40] chronic progressive EAE in the Biozzi-ABH mouse,[39] in C57Bl/6 mice immunized with an MBP-PLP fusion protein[41] and following adoptive transfer of MOG-specific Th-17 T cells into C57Bl/6 mice.[42–44] However, little is known concerning the molecular mediators responsible for initiation and maintenance of such organized immune cell infiltrates and their role in the development of demyelinating and neurodegenerative pathology in the underlying CNS tissues. Our previous studies have demonstrated a close association between the formation of TLS in the SAS of the cerebral cortex and demyelinating and neurodegenerative pathology in the underlying GM of the multiple sclerosis brain, which is not reproduced by any of the EAE models.[6,10,45] To study this relationship, we have recently developed a novel model in the rat in which the levels of proinflammatory cytokines can be chronically and ectopically raised to pathological levels.[46] Given the potential role of LTα in both cellular cytotoxicity and TLS formation, here we aimed to show whether acute or chronically elevated levels of LTα in the SAS of the rat brain can result in meningeal TLS formation and subsequent demyelination and neuronal loss. Establishing the factors that may drive the formation of TLS in multiple sclerosis and their causal relationship to cortical pathology will open up an avenue for the development of an effective approach to slowing the progressive course of multiple sclerosis.

Materials and methods

Human tissue sample selection and immunohistochemistry

Post-mortem brain tissue was provided by the UK Multiple Sclerosis Tissue Bank at Imperial College London, which obtains tissue through a prospective donor scheme, approved by the National Research Ethics Committee (80/MREC09/31). The diagnosis of all multiple sclerosis cases was confirmed by a consultant neuropathologist according to published guidelines, as described previously.[3] Isolated meningeal tissue samples were dissected from eight control cases with no neurological disease and 20 secondary progressive multiple sclerosis cases (SPMS).[12] Details of each case are listed in Supplementary Table 1. Cases were classed as PM-MShigh or PM-MSlow based on numbers of haematoxylin-stained cell nuclei in two meningeal infiltrates and presence and extent of subpial GM demyelination, as described previously.[12]

Protein levels of LTα were determined in post-mortem CSF obtained at autopsy from 20 SPMS, 10 with high (PM-MShigh) and 10 with low (PM-MSlow) meningeal inflammation, and 10 healthy controls (details in Supplementary Table 1), using immune-assay Luminex technology (Bio-Plex ×200 System equipped with a magnetic workstation, BioRad). All samples were run undiluted, in duplicate in the same experiment and in two consecutive experiments, to verify the reproducibility and consistency of the results as previously described.[12]

Drug-naïve RRMS patients were screened at diagnosis by 3 T DIR-MRI and stratified into MSHigh ($n = 18$) and MSLow ($n = 13$) by the presence of at least 10 cortical lesions or <2 cortical lesions, respectively (Supplementary Table 2), as described for this patient cohort previously.[12] The control cohort ($n = 10$) consisted of subjects with non-inflammatory neurological disease.[12] CSF samples were acquired from these patients at least 2 months from the last relapse, according to the Consensus guidelines for CSF and Blood biobanking. Samples were centrifugated before storage of the supernatant at −80°C until use. Levels of LTα were assessed using immune-assay multiplex techniques on the Luminex technology (Bio-Plex ×200 system equipped with a magnetic workstation, BioRad), in the same way as the post-mortem samples.

Quantitative reverse transcription PCR

Meningeal tissue was isolated from post-mortem brain by manual dissection using a scalpel from up to 16 snap-frozen cortical blocks per multiple sclerosis and control case to give a total mass of 100–250 μg of tissue per case.[21] RNA was extracted using an RNeasy Lipid Tissue Mini Kit (Qiagen) and quantified by Nanodrop ND1000 spectrophotometer. For astrocyte and microglial cultures and rat cortical tissue, RNA was extracted using TRIzol followed by an RNAeasy Mini kit (Qiagen). Reverse transcription of 1 μg RNA per case to complimentary DNA (cDNA) was performed using a Quantitect Reverse Transcription Kit (Qiagen) with integrated genomic DNA removal. Prime Time quantitative polymerase chain reaction (qPCR) Assays (Integrated DNA Technologies) were used to quantify expression of LTα in human samples relative to the expression of two housekeeping genes (glyceraldehyde-3-phosphate dehydrogenase, GAPDH and Xpnpep1). Xpnpep1 is the most stable housekeeping gene in post-mortem CNS tissue, with no known associations with neuroinflammatory or degenerative pathologies.[47] For all rat tissue and cultured cells, PPIA (peptidyl-prolyl *cis–trans* isomerase A) and TOP1 (DNA topoisomerase 1) were used as housekeeping genes. Primers used for PCR with reverse transcription (RT–PCR) on astrocytes and microglia are listed in Supplementary Table 3. Reactions of 20 μl were performed in triplicate for each case on a Stratagene MXP4000 system (Agilent Technologies), with MxPro 2007 software. An inter-plate calibrator did not detect any significant inter-plate differences in efficiency between successive runs. The thermal profile was 95°C for 10 min, 50 cycles with a two-step program (95°C for 15 s, 60°C for 45 s). Changes in genes expression were calculated using the ΔΔCt method.

Lentiviral vector production

Lentiviral (LV) vectors expressing human LTα (LVLTα) or enhanced green fluorescent protein (LVGFP) were produced as described previously.[46] We used an HIV-1 transfer plasmid (326-pRRL-sincppt-CMV-eGFP-WPRE genome plasmid) that carries the human cytomegalovirus promoter (CMV) for lentiviral production. Complementary DNA sequences for human lymphotoxin-alpha

(LTα) were codon optimized for rat, including a 5′ Kozak sequence, and synthesized by Gene Art with Xba1 and Sal1 restriction sites (Life Sciences). The human transgene DNA fragments were excised by restriction digest with Xba1 and Sal1 before purification using preparative agarose gel electrophoresis. The eGFP was removed from the transfer plasmid by digestion with Xba1 and Sal1 and the transgene DNA fragments ligated in-frame using the same restriction sites.

Recombinant HIV-1 based lentiviruses were produced using four plasmid cotransfection of HEK-293T cells as described previously.[46] Briefly, HEK-293T cells were transfected with 15 μg vector plasmid (pRRLsincppt-CMV-LTα-WPRE or pRRLsincppt-CMV-GFP-WPRE), 15 μg of the packaging vector plasmids expressing the HIV-1 gag/pol gene (pMD2-LgRRE), 3 μg of HIV-1 Rev (pRSV-Rev) and 5.1 μg VSV-G envelope plasmids (pMD2-VSV-G) following the addition of 2 mol/l CaCl₂. Lentivirus was concentrated from supernatant using ultracentrifugation and the genome copy number was calculated using the Clontech Lenti-X RT–qPCR Titration kit (Takara).

Transduction of HEK cells

HEK-293T cells, obtained from ATCC, were maintained at 37°C, in a 5% CO_2 environment and cultured in Dulbecco's modified Eagle's medium (Sigma), supplemented with 10% newborn calf serum (Heat inactivated, Sigma), 2 mM penicillin/streptomycin and 2 mM L-glutamine (Sigma). Hek-293 T cells were plated in 24-well plates for 24 h before transduction with LVLTα or LVGFP at multiplicities of infection of 5, 10, 20, 35 and 50 and the supernatant harvested after 24 and 48 h.

Transduction of primary meningeal cultures

Primary meningeal cultures were prepared from P2 Sprague-Dawley pups. Briefly, the meninges were dissected from the surface of the cortex and digested with papain and DNAse. Cells were plated on poly-L-lysine-coated eight-well chamber slides or 24-well plates (Corning) and grown in DMEM/F12 (Sigma) supplemented with 10% calf serum, 1% penicillin/streptomycin and 1% L-glutamine (Sigma). After 1 week in culture, cells were transduced at various multiplicities of infection with LVLTα, or LVGFP and the supernatant harvested after 72 and 96 h and 7 days. Enzyme-linked immunosorbent assay for human LTα was performed in triplicate using the DUOset ELISA kit (DY210, R&D Systems). Protein was extracted from transfected meningeal cells using RIPA buffer (R0278, Sigma) and run on a western blot at 20 μl per well. Protein was stained with an antibody specific for human LTα to confirm expression.

For gene expression analysis of meningeal cells, 1×10^5 cells were plated in six-well plates and treated with 100 ng recombinant human LTα. RNA was extracted using TRIzol reagent according to the manufacturer's instructions and 1 μl of RNA converted to cDNA using High-capacity cDNA reverse transcription kit (ThermoFisher). Prime Time qPCR Assays (Integrated DNA Technologies) were used to quantify expression of LTα relative to the expression of two housekeeping genes (CYC1 and TOP1). Reactions of 20 μl in PowerUp SYBR green (ThermoFisher) were performed in triplicate for each case on a Stratagene MXP4000 system (Agilent Technologies) with MxPro 2007 software. The thermal profile was 95°C for 10 min, 40 cycles with a two-step program (95°C for 5 s, 60°C for 30 s). Changes in gene expression were calculated using the ΔΔCt method.

Immunofluorescence of primary meningeal cells

For immunofluorescence of transfected meningeal cells grown in eight-well chamber slides, cells were fixed with cold 4% PFA for 1 h at room temperature. After fixation, cells were incubated with 0.1 M PBS-0.1% triton-X-100 for 1 h. Primary antibodies were added at their corresponding working concentration for 1 h at room temperature. After primary antibody incubation, cells were thoroughly rinsed in 0.1 M PBS, three times for 10 min each. After rinsing, cells were incubated with appropriate secondary antibody conjugated to the appropriate fluorophore for 1 h at room temperature. The cells were rinsed in 0.1 M PBS (three times, 10 min each) and dH$_2$O, and counterstained with DAPI (diluted in 1:10 000). Last, the tissues were mounted with Vectashield Antifade Mountant and cover-slipped (24 × 50 mm, VWR, International).

Primary astrocytes and microglia

Astrocyte and microglial cultures were produced from cerebral cortex by microdissection from 2-day old Sprague-Dawley rat pups. Tissue was digested in papain before being plated on poly-D-lysine and laminin-coated plates, and grown in high glucose DMEM with 10% foetal bovine serum. After 21 days in culture, microglia were removed by shaking for 1 h at 300 rpm and plated in 24-well plates at a concentration of 2×10^5 cells/well. Microglia were grown in Advanced RPMI medium (Gibco) supplemented with 10% foetal bovine serum and 2 mM L-glutamine. Astrocytes were shaken for a further 24 h to removed remaining microglia and oligodendrocyte progenitor cells. Astrocytes were then passaged using accutase and replated at 3×10^5 cells/24 well and left for 24 h in high glucose DMEM medium. For experiments where cells were treated with recombinant LTα (full length human LTα abcam ab243774, suspended in PBS), both astrocyte and microglial cultures were treated with 50 μM recombinant human LTα for 2 h, before their respective media were changed again for fresh. For controls the medium was changed as before for the 2 h treatment period, then changed again for fresh. Cells were then kept for a further 24 h before harvesting for RNA extraction. For conditioned medium experiments, following 2 h of cytokine stimulation of microglia, the medium was replaced with fresh and they were left for a further 24 h. Supernatant from either control or LTα treated microglia was harvested after 24 h, passed through a 0.2 μm filter before being diluted 1:2 in astrocyte medium and added to astrocyte cultures for 24 h. For CSF-treated cells, 50 μl CSF from each of two 28 dpi rats was mixed with 1.5 ml of culture medium (1:30 dilution) to produce sufficient for three wells (500 μl per well). CSF from six IFA and six MOG + IFA animals was divided into pairs to give a total of three treated astrocyte cultures for IFA and three for MOG + IFA, with triplicates for each pair. Cells were treated with CSF containing medium for 24 h before harvesting.

Animals

All *in vivo* procedures were performed under UK Home Office approval. Eight to ten-week-old female Dark Agouti rats (140–160 g) were obtained from Janvier (France) and kept in groups of four in a 12 h light/dark cycle with food and water provided *ad libitum*. A total of 92 animals were used for all experiments.

Induction of subclinical experimental autoimmune encephalomyelitis

Subclinical MOG-induced EAE was induced as described previously.[21,46] Rats were anaesthetized with isofluorane and immunized intradermally at the base of the tail (dorsal aspect) with 5 μg of recombinant mouse MOG (amino acids 1–119, corresponding to the external Ig-like domain) diluted in sterile PBS and emulsified in an equal volume of incomplete Freund's adjuvant (IFA, Sigma; total volume 100 μl per rat). IFA-only control rats were immunized with PBS emulsified in an equal volume of IFA without the addition of MOG protein, and naïve age-matched control rats (n = 6) received no treatment. For all groups n was 5 to 7 animals, randomly assigned to experimental groups. All animals were weighed, examined and clinically scored on a daily basis according to a scoring system to define the level of neurological deficit, as described previously.[48] This dose of recombinant MOG protein has been previously shown to elicit only subclinical EAE in Dark Agouti rats of similar age and weight,[21] with production of peripheral anti-MOG IgG1 and IgG2a antibody titres previously confirmed to be present in MOG-immunized but not IFA-immunized animals.[46]

Subarachnoid injection of cytokines and lentiviral vectors

Following immunization, stereotaxic injections of recombinant cytokines or lentiviral (LV) vectors into the SAS were performed under isofluorane anaesthesia at 20–23 days post-immunization, or at an equivalent time-point in age-matched naïve control animals. A 5 mm hole was drilled in the skull at 0.9 mm caudal to bregma at the level of the motor cortex. A finely calibrated pulled glass capillary needle attached to a 26S fixed needle Hamilton syringe (10 μl) was lowered to a depth of 2.3 mm ventral to the dural membrane. The cytokines or lentiviral vectors were infused at a rate of 0.2 μl/min over a period of 20 min (total volume injected 2–4 μl). Monastral blue (copper II phthalocyanine-tetrasulfonic acid tetrasodium salt; Sigma-Aldrich) was added as a tracer to determine the location of the injections, and resulted in no pathology, as confirmed by previous studies.[49–51] For lentiviral injections, 4 μl of lentiviral vector solution diluted in TSSM with 0.5 mM monastral blue at a total of 5×10^8 genomic copies (GC) for LTα and GFP was injected at a rate of 0.2 μl/min. For recombinant cytokine injections, control animals received an injection of sterile PBS 0.5% BSA (n = 5). Recombinant human lymphotoxin-alpha [hLTα, reconstituted in 0.1% (w/v) BSA in sterile PBS; Peprotech] and recombinant rat IFNγ [reconstituted in pH 8 sodium phosphate (10 mM; Sigma-Aldrich)] were diluted to the required concentrations (LTα 1 μg + IFNγ 75 ng per injection) and injected at a total volume 2 μl per rat. For all injections, the glass capillary needle was left in place for 10 min after the injection to allow diffusion of the injected solution away from the injection site before slow retraction of the capillary. A group of age-matched naïve rats that received no immunization or SAS injections, provided an additional control group (n = 6).

Tissue processing and CSF analysis

At the termination of the experiment, rats were killed by intraperitoneal injection of 200 mg/kg of sodium pentobarbitone and a 50–100 μl CSF sample taken from the cisterna magna using a 26G needle (Hamilton) before cessation of breathing, with the animal on a stereotaxic frame. Animals were perfused with 100 ml of PBS followed by 400 ml of 4% PFA through the left ventricle at 3, 7, 14, 21, 28, 56 and 90 days post viral vector injection. Brains were removed and post-fixed in 4% PFA (4 h at room temperature), before cryoprotection in 30% sucrose solution (w/v in PBS) for 72 h until equilibrated. Brains were embedded in optimal cutting temperature compound (Tissue-Tek, Sakura) and frozen in isopentane on

dry ice. Coronal cryosections (10 μm) were stored at −20°C before performing immunofluorescence. Protein expression for the expressed human LTα transgene was measured in snap-frozen rat CSF using a human TNFβ/TNFSF1 Quantikine ELISA kit (DTB00, R&D systems) as per the manufacturer's instructions.

Immunohistochemistry and immunofluorescence

Immunofluorescence was performed as previously described.[46] For immunohistochemistry snap-frozen sections were fixed with cold-methanol (4°C) for 10 min and blocked with 10% normal horse serum, followed by overnight incubation with primary antibody and then incubated with ImmPRESS HRP-conjugated secondary antibodies (Vector laboratories). For single IHC, slides were visualized with ImmPACT-DAB (Vector Laboratories) as the chromogen. Dual-colour IHC was performed by sequential staining, followed by detection with ImmPACT-DAB, incubation with the second primary antibody and detected using the ABC-alkaline phosphatase detection system with Vector blue as substrate. The primary antibodies used were: mouse anti-MOG (clone Y10, Prof Reynolds, Imperial College London, UK); rabbit anti-MBP (Polyclonal, Merck); mouse anti-neurofilament-H protein (clone NE14; Merck); rabbit anti-IBA1 (Polyclonal IgG, Wako Pure Chemical Corporation); rabbit anti-glial fibrillary acidic protein (GFAP) (Polyclonal, Dako Agilent); mouse anti-NeuN (clone A60, Merck); mouse anti-CD79a (ThermoFisher); mouse anti-CD4 (AbD Serotec); mouse anti-CD8 (AbD Serotec); goat anti-human LTA (R&D systems); rabbit anti-laminin (Wako); rabbit anti-cleaved caspase-3 (Cell Signalling); goat anti-CXCL13 (R&D systems); mouse anti-CCL21 (R&D systems); mouse anti-CCL19 (R&D systems); mouse anti-CXCL12 (monoclonal, Sigma); rabbit anti-CXCR4 (Sigma); goat anti-LTBR (polyclonal goat, R&D); rabbit anti-Ki67 (Santa-Cruz); rabbit anti-CD3 (DAKO); rabbit anti-IgG (R&D); rabbit anti-laminin (Novusbio); mouse anti-MadCam (monoclonal mouse, R&D systems); mouse anti-CNPase (Millipore); rabbit anti-CXCR5 (Abcam), rabbit anti-podoplanin (Abcam); mouse anti-CCR7 (mouse monoclonal, R&D systems); rabbit anti-pMLKL (Cell Signalling); and mouse anti-HuC/D (Millipore).

All the secondary antibodies used for immunofluorescence were purchased from ThermoFisher Scientific: Alexa Fluor 546 goat Anti-Mouse IgG (H + L), Alexa Fluor 546 goat Anti-Rabbit IgG(H + L), Alexa Fluor 488 goat Anti-Mouse IgG (H + L) Fluor 488 goat Anti-Rabbit IgG (H + L), Alexa Fluor 488 goat Anti-Mouse IgG1, Alexa Fluor 546 goat Anti-Mouse IgG1, Alexa Fluor 647 goat Anti-Mouse IgG1, Alexa Fluor 488 goat Anti-Mouse IgG2b, Alexa Fluor 647 goat Anti-Mouse IgG2b, Alexa Fluor 488 Streptavidin, Alexa Fluor 546 Streptavidin and Alexa Fluor 647 Streptavidin. To couple with Alexa Fluor labelled Streptavidin, the following biotinylated antibodies were used from Vector Laboratories: biotinylated goat anti-Rabbit IgG (H + L), biotinylated Horse anti-Mouse IgG (H + L) and biotinylated goat anti-Mouse IgG2a (Life Technologies, ThermoFisher Scientific).

Image acquisition

Immunostained sections were viewed with either an epifluorescence Olympus BX63 scanning microscope or a SP8 Leica confocal microscope for the rat sections and a Zeiss Axioscope 5 for the human sections. Tiled digital images were obtained on the Olympus BX63 microscope at ×10 or ×20 magnification and coded for blinded analysis using ImageJ software (NIH, Maryland, USA). Higher magnification images were acquired on the Leica confocal microscope at ×60 magnification.

For each animal, immunofluorescence tiled images were acquired from 4×10 μm sections stained with anti-MOG antibody to quantify demyelination. Cortical and midline layers were delineated as regions of interest and automated Otsu thresholding was used to calculate the percentage area of regions of interest stained by the MOG antibody. For the recombinant cytokine study, thresholding was also used to calculate the area of IBA1 immunoreactivity (IR). CNPase expressing cells were quantified manually using the cell counting tool in ImageJ. For quantification of meningeal inflammation, images of the length of the sagittal sulcus were acquired at ×20. DAPI staining was used to calculate the area of the SAS from the base of the sagittal sulcus to the position of the lateral blood vessels visible in the meninges. Meningeal immune cell numbers were counted manually for CD4-, CD8- and CD79a-expressing cells using the cell counting tool in ImageJ software and expressed as cells/mm^2, from 4×10 μm sequential sections spanning an 80 μm distance in the anterior/posterior plane. For parenchymal immune cells, a boundary of 200 μm in width was drawn around the midline and cells within the regions of interest were quantified manually.

For both neuronal and microglial numbers, regions of interest were drawn that outlined the cortical layers or midline regions using ImageJ. Cortical layers were determined using costaining with DAPI and GluR2/3 to identify different cortical regions.[21,46] Cortical regions began from the lateral vessels in the meninges at the top of the sagittal sulcus and extended the breadth of the cortex to the rostral regions. NeuN$^+$ and IBA1$^+$ cell numbers were counted manually at ×20 magnification using the ImageJ cell counter tool. The total number of cells for all the counts was then divided by the total area of the region of interest to give the total cells/mm^2. For neurons and microglia, the number of cells was calculated from four sections per animal that were spaced 10 μm apart covering a total distance of 80 μm per animal.

Statistical analysis

Graphpad Prism8 statistical software (La Jolla, CA, USA) was used in all cases to present the data and to conduct statistical analysis. All data on graphs are expressed as mean ± SEM, except for PCR data that are shown as ΔΔCT with standard errors. Group comparisons for cell quantifications were analysed by one-way ANOVA with a Tukey test for multiple comparisons.

Data availability

All data are available within the paper, the figures and the supplementary data.

Results

Expression of LTα in the CSF and meninges of patients with multiple sclerosis

A cohort of recently diagnosed drug-naïve RRMS patients were grouped on the basis of the presence of at least 10 cortical lesions (MSHigh) or <2 lesions (MSLow) from 3D DIR-MRI imaging (cohort described previously by Magliozzi et al.[12]). Significantly increased levels of LTα were present in the CSF of the MSHigh patient group compared to controls and the MSLow patient group (Fig. 1A).

In a similar way, significantly elevated LTα protein levels (Fig. 1B) were found in the CSF of the high inflammation post-mortem SPMS brains (called PM-MSHigh: >60% GM demyelination and high levels of immune cell infiltration[12]), compared to both

controls and the low inflammation post-mortem SPMS group (called PM-MSLow: <40% GM demyelination and a low density of diffuse meningeal inflammation). Levels of LTα mRNA in the post-mortem meninges were also significantly increased in SPMS brains compared to controls (3.2 ± 1.2-fold; $P = 0.028$) (Fig. 1C). Immunostaining for LTα showed cytoplasmic staining in cells within the meningeal infiltrates (Fig. 1D), many of which costained for the pan T-cell marker CD3 (Fig. 1E–G). In addition, a population of CD3 negative cells expressing LTα were also present in the infiltrates (Fig. 1E). Immunohistochemistry for LTβR showed a diffuse pattern of reticular-like staining throughout the meningeal infiltrates (Fig. 1H).

Meningeal inflammation after recombinant LTα/IFNγ injection in rats

To reproduce the increased CSF levels of LTα seen in multiple sclerosis and the subsequent meningeal pathology, we used a novel model developed in our laboratory in which either recombinant cytokines or viral vectors carrying the cytokine genes were injected into the SAS of the sagittal sulcus of Dark Agouti rats.[21,46,52] To study the effects of an underlying autoimmune response against myelin, rats were immunized with rmMOG in IFA or IFA alone and then 20–23 days post-immunization were given an injection of recombinant hLTα and IFNγ into the SAS. Following the injection of recombinant cytokines into the SAS of Dark Agouti rats, the formation of extensive dense cellular infiltrates was observed down the entire depth of the sulcus and extending across the lateral surface of the cortex between 3 and 14 days following injection, with the greatest levels seen between 3 and 7 days, which was absent in controls that received only a PBS injection (Fig. 2A). The meningeal infiltrate was composed of predominantly CD4+ and CD8+ T cells and CD79a+ B cells (shown in Fig. 2B at 3 dpi). CD4+ and CD8+ T-cell numbers were highest at 3 dpi and decreased thereafter, until they were almost absent by 14 days (Fig. 2C). At both 3 and 7 dpi the numbers of CD4+ cells were roughly twice the numbers of CD8+ T cells (Fig. 2C). Infiltration of CD79a+ B cells was maximal at 7 days post-injection with numbers staying significantly high at 14 and 21 dpi (Fig. 2C). Whereas CD4+ and CD8+ T cells were roughly evenly distributed throughout the SAS with no observable organization, CD79a+ B cells often formed discrete dense clusters of cells as early as 3–7 days (Supplementary Fig. 1A). Approximately 65% of CD79a+ B cells coexpressed the proliferation marker Ki67 at 3 dpi, suggesting local clonal expansion, with the percentage of CD79a+ Ki67+ cells decreasing over time (Fig. 2D and E; Supplementary Fig. 1B).

Demyelination and microglial activation after acute recombinant LTα/IFNγ injection in rats immunized with MOG

Injection of PBS into the SAS of control animals, either naïve or those immunized with MOG + IFA (Fig. 2F and G) or IFA only (not shown), did not result in any demyelination or activation of microglia. Rats immunized with low dose rmMOG in IFA that also received a stereotaxic injection of human 1 μg LTα and 75 ng IFNγ recombinant proteins into the SAS exhibited subpial demyelination of the upper cortical layers (Fig. 2H and I) and midline layers as early as 3 dpi (Supplementary Fig. 1G), which became even more extensive at 7 dpi (Fig. 2J and Supplementary Fig. 1H) and began to resolve at 14 dpi (Fig. 2L and Supplementary Fig. 1I) and was accompanied by substantial IBA1+ microglial activation (Fig. 2H–M). Demyelination extended from the corpus callosum boundary of

the sagittal sulcus to the dorsal surface of the cortex and laterally from the midline across the subpial surface of the cortex through to rostral regions. By 21 dpi there was very little apparent loss of MOG staining with only small patches of loss seen mostly in midline regions (Fig. 2N and Supplementary Fig. 1J), with negligible IBA1+ microglial activation, suggesting that remyelination had occurred. Quantification of the loss of MOG staining demonstrated that demyelination was greatest at 7 dpi when compared to PBS control animals with less demyelination at 3 and 14 dpi in midline layer I (Supplementary Fig. 1C) and midline layer II–III (Supplementary Fig. 1D). A similar pattern was seen in cortical layers I–IV (Fig. 2P) with significantly less MOG+ myelin staining at 7 dpi ($15.2 \pm 2.2\%$) than at 3 dpi ($23.2 \pm 3.9\%$) compared to PBS injected control animals. By 21 dpi there was no quantifiable demyelination in the cortical layers (Fig. 2P), but still some loss of MOG staining in midline regions (Supplementary Fig. 1C and D). Quantification of IBA1+ immunofluorescence showed levels peaked at 7 dpi in cortical (Fig. 2Q) and midline (Supplementary Fig. 1E) layers, corresponding to the peak in demyelination, but were not significantly different from PBS animals by 14–21 dpi.

Expression of the LTα transgene

To study the chronic effects of increased LTα expression by cells in the meningeal space, we developed a high titre viral vector. Primary meningeal cells could be 100% transduced with the lentiviral vectors for LTα and GFP, demonstrating a good tropism for the virus (Supplementary Fig. 2A–F) with no obvious toxicity (Supplementary Fig. 2G). Transduced meningeal cells continued to produce transgenic protein and mRNA at increasing levels for several days (Supplementary Fig. 2K and L). Rats were then immunized with MOG + IFA or IFA only and after 20–23 days of chronic expression of LTα was induced by injection into the SAS of the lentiviral vector carrying the human LTα gene. Following stereotaxic injection into the SAS of the sagittal sulcus, as indicated by the presence of monastral blue dye at the injection site, mRNA for the LTα transgene was highly expressed at 90 days after injection in meninges dissected from near the injection site (Fig. 3A). Meningeal cells lining the sagittal sulcus were successfully transduced, as shown by the expression of GFP (Fig. 3B). Strong GFP expression could also be detected in meningeal cells lining the outer surface of the cortex. Immunofluorescence with anti-human LTα antibody demonstrated high levels of expression of the human LTα transgene in transduced meningeal cells down the sagittal sulcus at 28 and 90 dpi in both animals that were immunized with MOG + IFA or IFA only (Fig. 3C, illustrated here for MOG-immunized animals). Protein expression from the LTα transgene was also detectable in CSF samples and maintained at 28 and 90 days, while levels were undetectable in GFP vector-injected animals (Fig. 3D). Human LTα protein was expressed at high levels in tissue taken from around the injection site and was also present at low levels in surrounding cortical, but not cerebellar, tissue, suggesting some transduction in the cortex, possibly via diffusion down perivascular spaces (Fig. 3E).

Meningeal inflammation after LTα overexpression in the subarachnoid space

Substantial meningeal infiltrates developed in LTα lentiviral vector-injected animals, completely filling the midline SAS by 28 dpi and were maintained until at least 90 dpi (Fig. 4A). No qualitative difference was seen between IFA only and IFA + MOG-immunized animals. CD4+ and CD8+ T cells were roughly evenly distributed
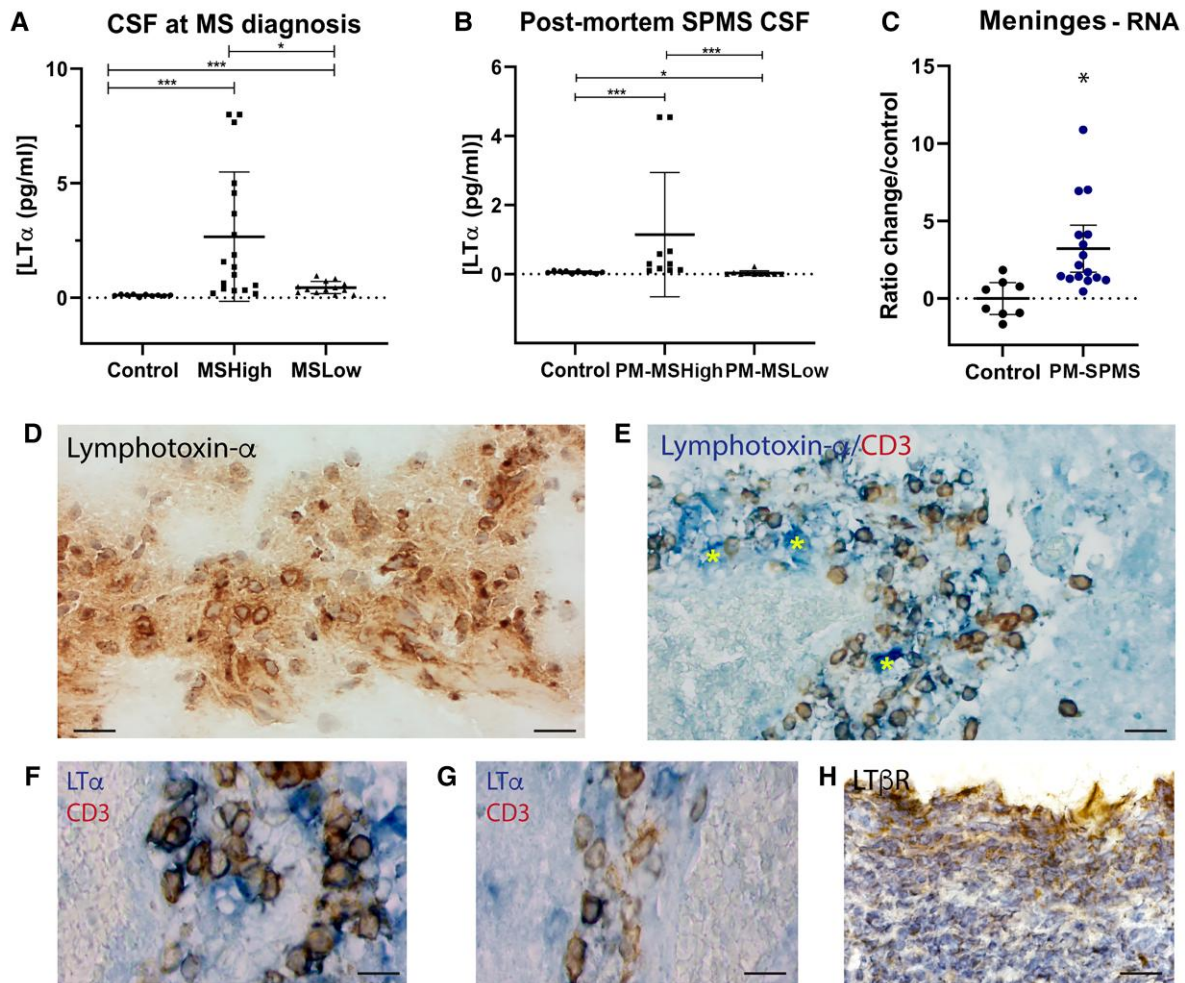
Figure 1 Analysis of the levels of LTα gene transcript and protein. (**A**) Levels of LTα measured in diagnostic CSF samples from 10 non-inflammatory neurological controls, 18 MSHigh and 13 MSLow cases by Bio-plex analysis. The number of cortical lesions on 3D DIR-MRI was used to stratify naïve patients with multiple sclerosis as MSHigh (>10 cortical lesions) or MSlow inflammation (<2 cortical lesions). (**B**) LTα protein levels in post-mortem CSF from 10 PM-MSHigh, 10 PM-MSLow and 10 control cases, measured by electrochemoluminescence (MSD). SPMS post-mortem cases were classed as PM-MSHigh or PM-MSLow based on the degree of immune cell infiltration in the meninges, determined by numbers of haematoxylin-stained nuclei in the infiltrate. (**C**) LTα gene transcript levels in meninges dissected from post-mortem tissue blocks of 16 SPMS cases and eight controls, determined by QPCR. Graph shows the fold change in mRNA levels in multiple sclerosis versus control. (**D**) Immunostaining for LTα in meningeal aggregates shows cytoplasmic staining in numerous cells in meningeal infiltrates. Scale bar = 50 μm. (**E**) Costaining for LTα (blue) and CD3 (brown) in meninges shows the presence of significant numbers of CD3$^+$ LTα$^+$ T cells, together with some LTα expressing cells that are not CD3$^+$ (yellow stars). Scale bar = 50 μm. (**F** and **G**) LTα (blue) and CD3 (brown) costaining at higher magnification. Scale bar = 20 μm. (**H**) Immunostaining for LTβR in meningeal aggregates shows a reticular-like staining. Statistics: (**A** and **B**) one- way analysis of variance with a Tukey *post hoc* test. $^*P < 0.05$, $^{***}P < 0.001$. (**C**) t-test on ΔCt data. $^*P < 0.05$.

throughout the space, whereas CD79a$^+$ B cells tended to cluster more (Fig. 4B). IBA1$^+$ myeloid cells were also present throughout the aggregates. Quantification of CD4$^+$ and CD8$^+$ T-cell numbers showed no significant difference in numbers between IFA only and IFA + MOG animals at both 28 and 90 dpi (Fig. 4C and D), with approximately equal numbers of CD8$^+$ and CD4$^+$ T cells. Although numbers of T cells were lower at 90 dpi, this still represented substantial infiltration. There was no difference in the number of CD79a$^+$ B cells between IFA or IFA + MOG animals at 28 or 90 dpi (Fig. 4E) and numbers were similar to both CD4$^+$ and CD8$^+$ T cells. Similar to the animals injected with recombinant cytokines, after viral vector injection, CD79a$^+$ B cells formed into densely packed focal clusters (Fig. 4F), with immunoglobulin-expressing plasma cells sparsely distributed in the same areas (Fig. 4G). Few or no CD8$^+$ or CD4 T cells were present within these CD79a$^+$ clusters and a proportion of CD79a$^+$ cells were proliferating at both time points, as demonstrated by coexpression with Ki67 (Fig. 4H). The percentage of

Ki67$^+$ B cells was stable between 28 and 90 dpi and was not different between MOG + IFA and IFA-only animals, suggesting a consistent level of B-cell proliferation that was not driven by the anti-MOG immune response (Fig. 4I and J). A very small number of CD8$^+$ cells were present in the surrounding cortical parenchyma of both IFA only and MOG + IFA animals (Fig. 4K and L), whereas no CD4 + cells were seen in this location (Fig. 4K). Large aggregates of infiltrating cells were also found along the lateral surface of the cortex, composed of CD4$^+$ and CD8$^+$ T cells (Fig. 4M) and CD79a$^+$ B cells (Fig. 4N), and were present as T-cell rich regions and B-cell aggregates (Fig. 4O).

Tertiary lymphoid structures in the meninges

The segregation of immune cells in the meninges into T-cell rich regions and large B-cell aggregates with ongoing proliferation was suggestive of TLS formation. Therefore, we further analysed
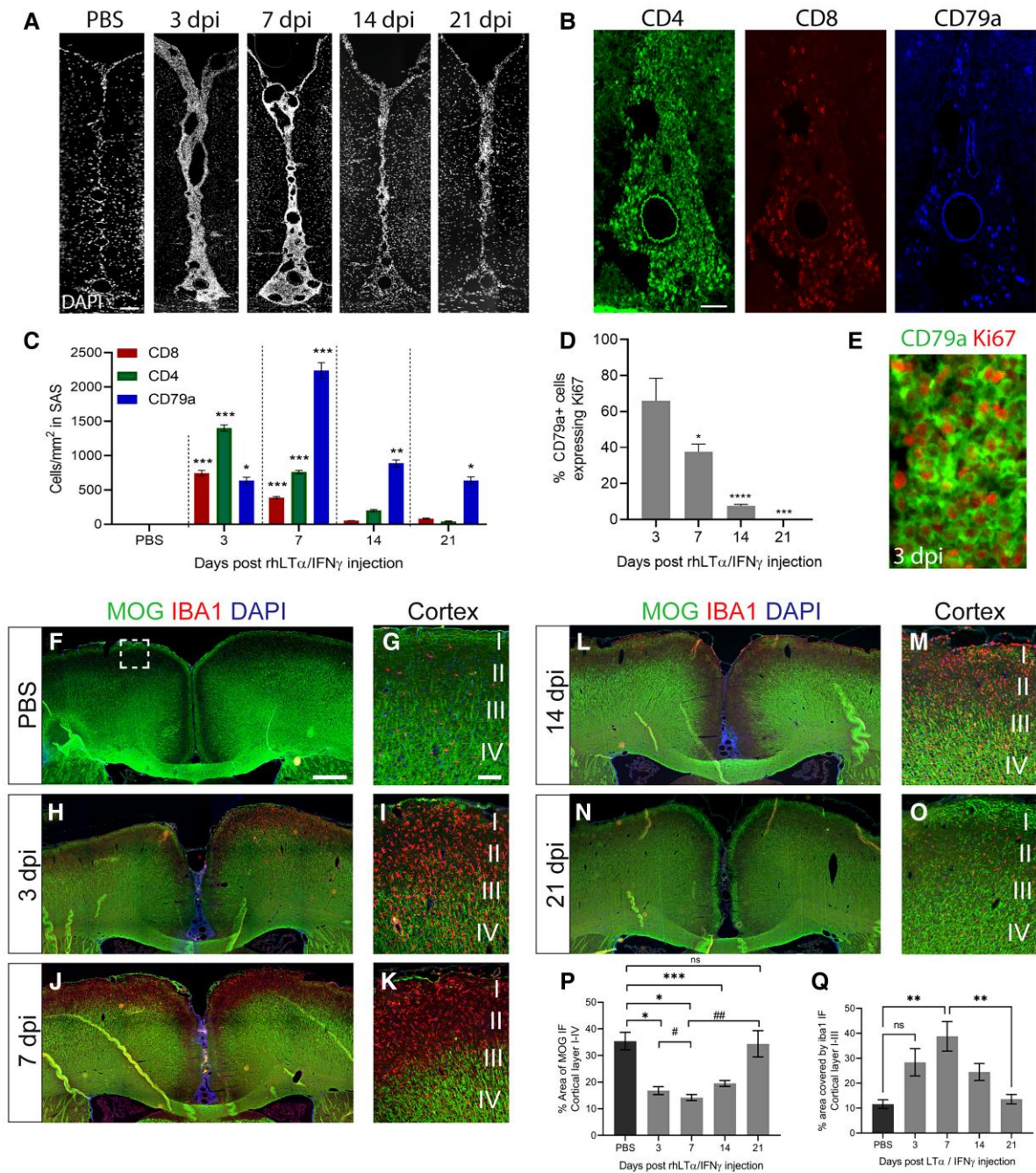
Figure 2 Demyelination and microglial activation after acute cytokine injection in rats immunized with rmMOG. (A) Recombinant LTα/IFNγ injection into the SAS led to the formation of large dense infiltrates of cells the length of the sagittal sulcus and across the surface of the cortex, visualized here at ×4 magnification by DAPI immunostaining. Injection of PBS did not lead to any infiltration. Scale bar = 100 μm. **(B)** Representative images of CD4, CD8 and CD79a immunofluorescence from sequential sections at 3 dpi post-injection of cytokines. Scale bar = 50 μm. **(C)** Quantification of CD4^{+}, CD8+ and CD79a+ cell numbers in the SAS expressed as cells/mm^{2}. Both CD4^{+} and CD8^{+} numbers were maximal at 3 dpi with CD4^{+} cell number 104% higher than CD8^{+}. Numbers at 14 and 21 dpi were not significantly increased compared to PBS injected. Maximal infiltration of CD79a^{+} B cells was seen at 7 dpi and was significantly higher than PBS controls at 3, 7, 14 and 21 dpi ($n = 3$–4 per group). $^*P < 0.05$; $^{**}P < 0.01$, $^{***}P < 0.001$ LTα/IFNγ versus PBS control. **(D and E)** Following LTα/IFNγ injection a proportion of CD79a^{+} cells (green) were positive for the proliferation marker Ki67 (red), scale bar = 100 μm. At 3 dpi 65% of cells were double positive ($n = 4$), significantly decreasing to 37.7% at 7 dpi ($n = 4$), 7.5% at 14 dpi ($n = 3$) and 0.07% at 21 dpi ($n = 3$). $^*P < 0.05$, $^{***}P < 0.001$, $^{****}P < 0.0001$ compared to 3 dpi. **(F–O)** Immunofluorescence for MOG and the microglial marker IBA1 in rmMOG-immunized rats injected with PBS **(F and G)** or 1μg LTα/75 ng IFNγ recombinant cytokines culled at 3 **(H and I)**, 7 **(J and K)**, 14 **(L and M)** and 21 **(N and O)** days post-cytokine injection (dpi), demonstrating the degree of demyelination and microglial activation at various times points. Cortex images are magnifications of the region shown by the boxed area in image **F**. Numbers I-IV represent the location of the cortical layers. Scale bars: **F, H, J, L, N** = 500 μm; **G, I, K, M, O** = 50 μm. **(P)** Quantification of subpial demyelination at the injection site in layers I–IV, presented as the percentage area covered by MOG immunofluorescence (IF) ($n = 3$–4 each group). $^{**}P < 0.001$ LTα/IFNγ at 7 days versus PBS control. **(Q)** Measurement of the area covered by IBA1 immunofluorescence in cortical layers I–III. $^{**}P < 0.01$ LTα/IFNγ at 7 days versus PBS control and 21 days. Data are presented as the mean ± SEM. Statistics: $^*,^{#}P < 0.05$, $^{**},^{##}P < 0.01$, $^{***}P < 0.001$, one-way analysis of variance with a Tukey *post hoc* test.
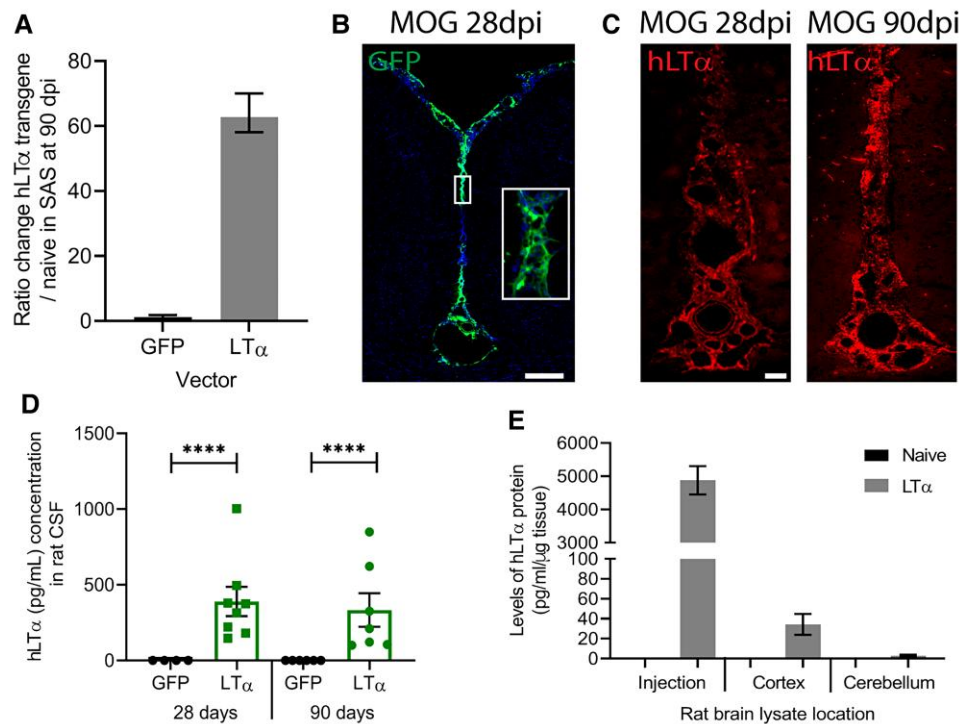
Figure 3 Primary meningeal cells transduced with lentiviral vector expressing human LTα. (**A**) Lentiviral vectors expressing eGFP, as a control, or LTα were injected into the sagittal sulcus. Following LVLTα injection, the human LTα transgene could be measured in the meninges dissected from rats at 90 dpi, but no expression was evident in the eGFP controls ($n = 3$ both groups). Data shown as ratio change of $2^{\Delta\Delta CT}$ for hLTα mRNA in LVGFP and LVLTα compared to naïve animals. (**B**) Significant transduction of meningeal cells with the lentiviral vectors could be demonstrated by expression of the GFP protein (green), the length of the SS and across the lateral surface of the cortex. Higher magnification image in box. (**C**) Immunostaining for hLTα (red) showed expression of the human LTα protein along the length of the SS that was present both at 28 and 90 dpi in MOG-immunized animals, demonstrating widespread transduction. (**D**) CSF samples were taken from the cisterna magna of injected animals shortly before perfusion at 28 and 90 dpi. hLTα levels were measured in CSF samples using electrochemiluminescence (MSD plates). hLTα could be detected at both 28 dpi (mean 389.6 pg/ml) and 90 dpi (333.6 pg/ml) at similar levels but was not present in LVGFP animals. Statistics: one-way analysis of variance with a Tukey *post hoc* test. ****$P < 0.0001$. (**D**) Quantification of hLTα protein levels by ELISA in tissue samples dissected from either naïve or LVLTα injected animals at 90 dpi at the site of injection and from the surrounding cerebral cortex and the cerebellum, demonstrating very local transduction.

the features of the areas of dense infiltration at 28 and 90 days postviral vector injection. A common feature was the presence of many channels of variable diameter at both 28 and 90 days, ranging from the size of large venules (Fig. 5A, green arrows; Fig. 4A and B) to smaller sized channels reminiscent of high endothelial venules (HEVs; Fig. 5A, red arrows). Staining for the mucosal addressin cell adhesion molecule (MAdCAM-1) revealed multiple MAdCAM-1⁺ vessels throughout the length of the sagittal sulcus (Fig. 5B). MAdCAM-1 was expressed by most of the larger lymphatic-like channels (Fig. 5C) and some smaller HEV-like vessels (Fig. 5D), and on cells with the morphology of slender squamous endothelium cells and on some process bearing cells (Fig. 5D). MAdCAM-1 expression by mature stromal organizer cells has been previously reported,[53] which this population of cells may represent. Many of the channels were also strongly laminin positive (Fig. 5E), particularly in the MOG-immunized animals, whereas the meningeal blood vessels were only weakly laminin positive. We were unable to further characterize the channels with other lymphatic markers as all currently available commercial antibodies for mouse and human proteins failed to react with the rat tissues. A dense matrix of stromal cells called fibroblastic reticular cells (FRC) are commonly found in the T-cell zone of TLS and express the markers podoplanin (gp38) and laminin. Podoplanin was highly expressed throughout the aggregates (Fig. 5F), particularly in regions that contained high

numbers of CD4 and CD8⁺ T cells. No difference in expression between IFA and MOG + IFA-immunized animals was seen, with staining for a dense podoplanin network seen in both (Fig. 5G). No staining was present in naïve or GFP vector-injected animals (not shown).

Binding of LTα homotrimers to the TNFR1/2 receptors and LTα/LTβ heterotrimers to the LTβR receptor induces expression of many chemokines involved in organization of the lymphoid environment, many of which are increased in multiple sclerosis CSF.[12] To investigate which chemokines are produced locally by resident meningeal cells, rat primary meningeal fibroblast cells were treated with 100 ng/ml of recombinant rat LTα. LTα treatment induced significant increases in gene expression for CCL19, CXCL13 and LTβR after 24 h (Fig. 5H). Transcript levels for BAFF, CXCL12 and CCL21 did not change significantly. RT–PCR on tissue dissected from the meninges of LVLTα injected animals at 28 dpi showed significant increases in the mRNA for CCL19, CCL21, CXCR4, CXCR5, CCR7, BAFF and MadCam, compared to GFP injected controls (Fig. 5I). CXCL13 showed the largest increase in mRNA transcript levels (Fig. 5J). Immunostaining for CXCL13 revealed expression throughout the meningeal aggregates (Fig. 5K) and at higher magnification displayed an FDC-like fibroblastic expression pattern with multiple thin processes extending throughout the infiltrates (Fig. 5L). In regions where strong CXCL13 expression was found, a population of follicular dendritic cells (FDC) could be stained for the rat FDC
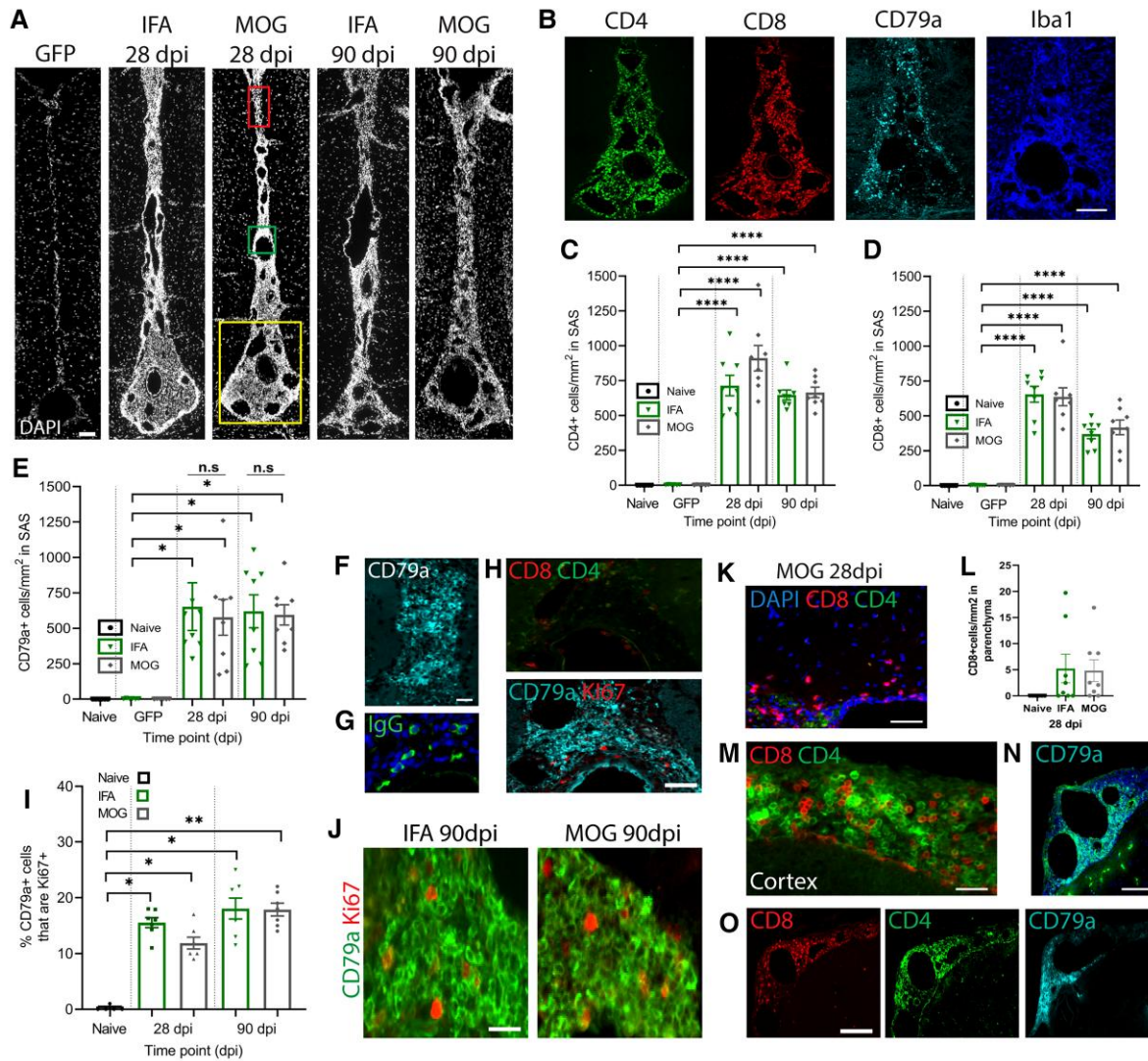
Figure 4 Overexpression of LTα in the SAS induces meningeal inflammation. (**A**) DAPI nuclear staining showing the accumulation of cells down the entire length of the sagittal sulcus in both IFA and MOG + IFA-immunized animals at 28 and 90 dpi, in comparison to the lack of cells in GFP vector animals. Scale bar = 200 µm. The yellow box represents location of images in **B**, the red box represents location for image in **F** and the green box represents location of images in **G–H**. (**B**) Immunostaining shows the presence of CD4^{+} and CD8^{+} T cells, CD79a^{+} B cells and IBA1^{+} myeloid cells within the dense infiltrates. Scale bar = 100 µm. (**C** and **D**) Quantification of the numbers of CD4^{+} (**C**) and CD8+ (**D**) cells/mm² down the length of the SAS in all animal groups. Data presented as mean ± SEM (*n* = 3–4 per group) (****P < 0.0001 LTα vector-injected compared to GFP control). (**E**) Quantification of CD79a^{+} B cells, expressed as cells/mm², in the sagittal sulcus shows substantially increased numbers compared to GFP control, but no significant difference between IFA and MOG[+] IFA-immunized animals and between 28 and 90 dpi (*P < 0.05, LTα vector-injected compared to GFP control). (**F**) Immunostaining of a cluster of CD79a^{+} cells within the SAS. (**G**) Ig expressing plasma cells are seen within CD79a^{+} B-cell clusters. (**H**) Regions where there were dense clusters of CD79a^{+} cells had very little presence of CD8 and CD4 cells, shown in a serial section. (**I**) The proportion of CD79a^{+} cells that were co-expressing the proliferation marker Ki67 (**J**) was not different between MOG + IFA and IFA-immunized animals at both 28 and 90 dpi (*P < 0.05, **P < 0.01 LTα vector-injected compared to naïve control). (**K**) A small proportion of CD8^{+} cells were seen in the underlying cortical parenchyma in both MOG + IFA and IFA-immunized animals, while CD4^{+} cells were absent (**L**). (**M**) Dense aggregates of cells were also present across the surface of the cortex (scale bar = 150 µm), containing CD8^{+} and CD4^{+} T cells (**M**) and clusters of CD79a^{+} B cells (**N**), particularly around large channels or vessels. (**O**) CD4^{+} and CD8^{+} T cells showed discrete localization patterns that were distinct from CD79a^{+} cells. Statistics: one-way analysis of variance with a Tukey *post hoc* test. Scale bars **H**, **M**, **N** = 100 µm. Scale bars **J**, **L** = 40 µm.

marker ED5 (Fig. 5M). FDCs were typically found in B-cell rich areas, but the more widespread diffuse expression could explain why some CD79a^{+} cells were found distributed throughout the aggregates, even if in small numbers compared to T cells (Fig. 4B). As expected, expression of the CXCL13 receptor, CXCR5, was found in close association within regions of high CXCL13 staining, along with clusters of CD79a^{+} B cells (Fig. 5N).

CXCL12^{+} expression, which provides a survival signal for incoming T cells, was present on process bearing cells throughout the meningeal infiltrates (Fig. 5O and P) together with its receptor CXCR4 (Fig. 5Q). Costaining of CCL21 and CXCL12 in T-cell rich regions revealed that they were expressed by distinct populations of cells (Fig. 5O), with no apparent coexpression of the two chemokines. CCL19 and CCL21 also showed differential expression patterns with minimal overlap (Fig. 5R and S). CD3^{+} cells were found in both CCL21 and CXCL12 rich regions. CCL21 could be seen in rounded amoeboid-like cells surrounding large channels (Fig. 5R, white arrows green channel). In contrast, CCL19 was seen in more
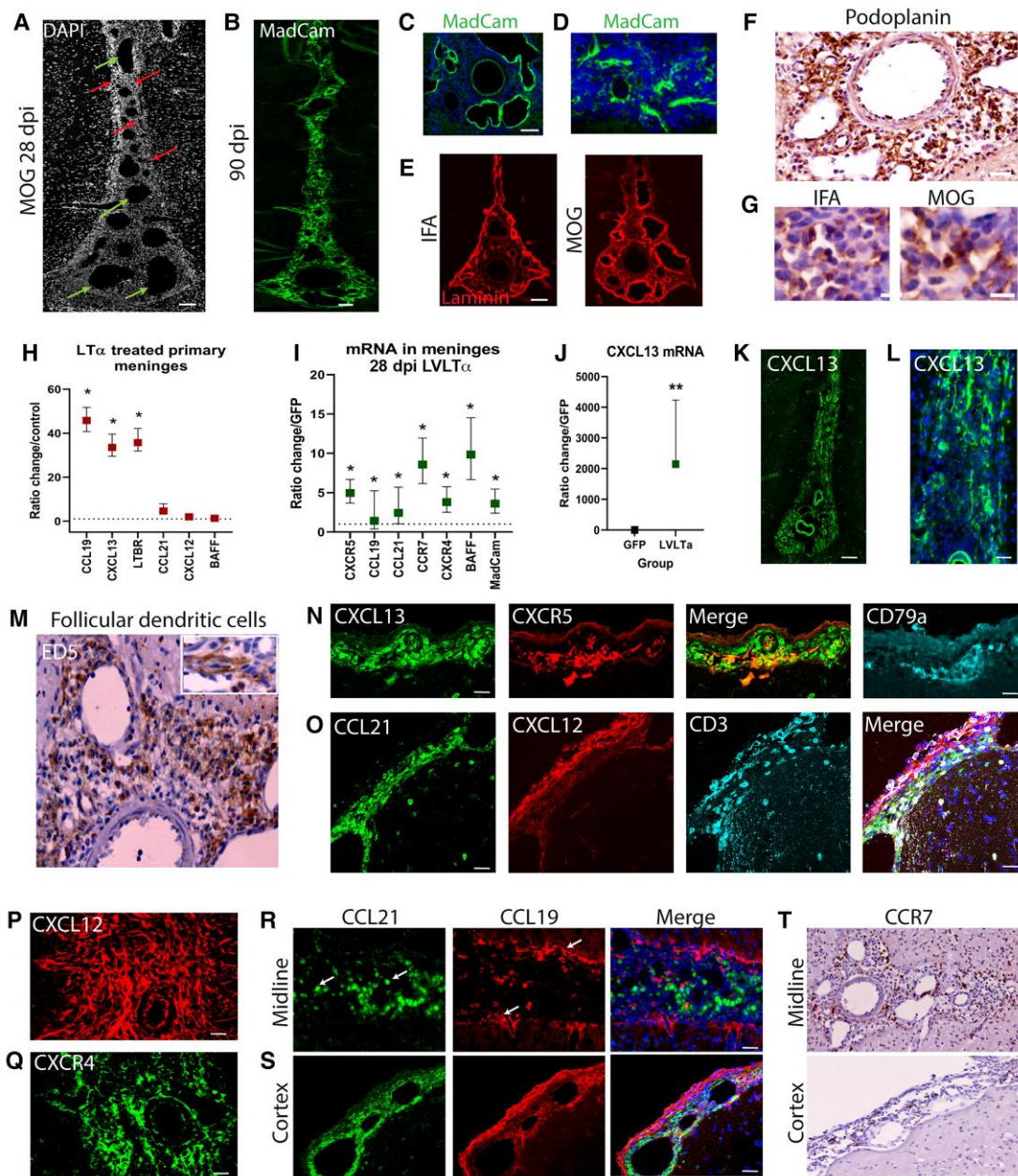
Figure 5 Presence of lymphatic channels in meningeal aggregates and expression of lymphoid chemokines by meningeal cells. (**A**) DAPI staining of meningeal aggregate at 28 dpi in a MOG-immunized animal showing the presence of multiple channels within the infiltrates that varied in size from small (red arrows) to very large, >100 µm in diameter (green arrows). (**B**) Immunostaining against MadCam-1 showed high expression the length of the SAS, particularly around the channels/vessels. Scale bar = 100 µm. (**C** and **D**) Higher magnification images show strong MadCaM immunofluorescence around large channels (**C**), as well as on a process bearing cellular network (**D**). (**E**) Laminin staining on the basement membranes surrounding the SAS, illustrating the glia limitans boundary, as well as around lymphatic vessels in both MOG + IFA and IFA-immunized animals at 28 dpi. Laminin immunostaining on blood vessels was much weaker. Scale bar = 100 µm. (**F**) Podoplanin immunohistochemistry shows a reticulum of staining throughout the immune cell infiltrates. Scale bar = 50 µm. (**G**) Higher magnification images of podoplanin immunoreactivity show that IFA and MOG + IFA-immunized animals express similar staining patterns in the cytoplasm and processes of meningeal cells. Scale bar = 20 µm. (**H**) Primary meningeal cells were treated with 100 ng/ml LTα for 24 h and changes in gene expression measured by RT–PCR. Ratio changes calculated for LTα treated over non-treated showed increased gene expression levels for CCL19, CXCL13 and LTβR. * P < 0.05 t-test on ΔΔCt values. (**I**) The cortical meninges were microdissected from 4 × 10 µm section from 28 dpi GFP or LVLTα injected animals for RNA extraction. Changes in mRNA levels for chemokines and receptors were measured by RT–PCR and shown here as cytokine vector treated compared to GFP control animals. *P < 0.05 t-test on ΔΔCt values. (**J**) In the dissected meninges, CXCL13 transcript showed the greatest fold change in cytokine versus GFP animals at 28 dpi. **P < 0.01 t-test on ΔΔCt values. (**K**) Immunostaining for CXCL13 at 28 dpi showed expression on blood vessels and lymphatic channels and on a network of cell processes throughout the immune cell infiltrate. Scale bar = 100 µm. (**L**) Higher magnification shows CXCL13+ staining on cells with follicular dendritic cell morphology with multiple thin processes. Scale bar = 40 µm. (**M**) IHC staining against ED5, a marker for FDC, showed a dense network of cells at 28 dpi. Inset box shows a higher magnification view. (**N**) CXCL13/CXCR5 double immunofluorescence and CD79a immunostaining on a serial section of cortical surface infiltrates. (**O**) Triple immunostaining for CCL21 and CXCL13 in regions with CD3+ T cells showed distinct localization patterns. (**P**) CXCL12 immunostaining was seen throughout the aggregates, together with expression of its CXCR4 receptor (**Q**). CCL21 and CCL19 double immunofluorescence in midline (**R**) and cortical aggregates (**S**). (**T**) Cells expressing CCR7 were found throughout the midline and cortical aggregates.

fibroblastic cells in the areas of infiltration along the edges of the sagittal sulcus (Fig. 5R, white arrows red channel) or cortical surface, in a pattern similar to that seen for CXCL12. Cells expressing the CCR7 receptor for CCL19 and CCL21 were present diffusely throughout the meningeal infiltrates (Fig. 5T).

Chronic LTα overexpression in the SAS causes subpial demyelination in rats immunized with low dose MOG

No observable demyelination was present at 28 dpi following injection of LTα vector in animals immunized with only IFA (Fig. 6A and B). At 90 dpi there was significant demyelination in the IFA-only group in the cortical layers I–III (Fig. 6D). In contrast, extensive subpial demyelination was found in midline and cortical regions at both 28 and 90 dpi in LTα viral vector-injected animals immunized with MOG + IFA (Fig. 6A and B), which reached into deeper cortical layers. Demyelination in MOG-immunized animals was significantly greater at 90 dpi than 28 dpi in both midline (Fig. 6C; $41.0 \pm 5.2\%$ of cortical GM remaining myelinated at 28 dpi versus $28.5 \pm 4.6\%$ at 90 dpi) and subcortical regions (Fig. 6D; $30.9 \pm 2.0\%$ remaining myelinated at 28 dpi versus $17.8 \pm 4.0\%$ at 90 dpi). GFP vector-injected control animals showed no quantifiable demyelination, regardless of their immunization status (Fig. 6C and D). Loss of MOG+ myelin extended from layer I directly beneath the pial surface down to layer III (Fig. 6E). In midline regions, loss of myelin extended from the midline into layer III (Fig. 6F). Loss of MBP immunostaining confirmed the presence of demyelination rather than a loss of the MOG protein specifically (Fig. 6G). We further confirmed the demyelination and accompanying loss of oligodendrocytes using immunostaining for CNPase, one of the earliest myelination-specific proteins expressed by both myelin and oligodendrocyte cell bodies (Fig. 6H–J). Whereas in IFA-only vector-injected animals there was weakened expression of CNPase, there was almost complete loss in MOG-immunized animals injected with the LTα vector (Fig. 6H). Quantification of CNPase+ oligodendrocytes at 90 dpi showed a significant loss in MOG-immunized animals compared to GFP controls (Fig. 6I). IFA animals only showed a non-significant small trend towards decreased numbers (Fig. 6I). Some CNPase+ cells colocalized with cleaved caspase-3 expression in demyelinated regions, suggesting they were being lost through apoptosis (Fig. 6J).

Widespread microglial and astrocyte activation in response to chronic LTα exposure

Microglial activation was extensive and widespread at 90 dpi in both IFA-only and IFA + MOG-immunized LTα vector-injected animals when compared to GFP vector-injected controls (Fig. 6K). In subpial cortical and midline regions, microglia showed a highly activated, ramified morphology, while in the deeper cortical layers V and VI directly above the corpus callosum they showed a more amoeboid morphology (Fig. 6L). Microglial numbers in LTα vector-injected animals were increased in the midline areas at both 28 and 90 dpi when compared to naïve and GFP controls, with no significant difference between MOG + IFA versus IFA-only immunized animals (Fig. 6M; 425 ± 37 cells/mm^2 in IFA versus 507 ± 74 cells/mm^2 in MOG animals at 90 dpi). In cortical layers IBA1+ cells were only significantly increased in MOG-immunized animals (Fig. 6N).

To determine whether astrocytes showed a reactive astrogliosis in response to chronic LTα overexpression, we stained for the astrocyte marker GFAP. Only low levels of immunostaining for GFAP were present throughout the cortical GM in both IFA and

MOG-immunized animals injected with the control GFP vector (Fig. 7A). In contrast, following injection of LVLTα, GFAP staining intensity was greatly increased in subpial cortical regions at both 28 and 90 dpi in both IFA and MOG + IFA-immunized animals, but not in deeper cortical layers III–V (Fig. 7A). The only obvious difference in GFAP staining between IFA-only and MOG + IFA LVLTα animals was an increased expression in the corpus callosum at 28 dpi in MOG immunized animals, a region that has some demyelination (Fig. 7A). In upper cortical regions of LVLTα injected animals, there was an upregulation of GFAP in a decreasing gradient, with strongest expression at the pial surface extending down to layer II (Fig. 7B). In the deeper cortical layer VI, there was strong upregulation of GFAP in areas in close proximity to the corpus callosum compared to GFP vector animals (Fig. 7B). Midline areas surrounding the SAS displayed intense GFAP staining, predominantly in subpial astrocytes (Fig. 7C). This was a different pattern of activation compared to microglia, which displayed a more homogenous pattern of activation across all cortical regions. This may reflect a more direct astrocyte reactivity to factors from the CSF. The activation mostly in subpial regions may be indicative of the depth that cytokines from the CSF can penetrate. LVGFP injection also led to a small increase in GFAP staining in midline regions suggesting the surgical procedure stimulates astrogliosis to a small degree (Fig. 7C). Quantification of GFAP+ cells showed significant increases in subpial midline layers (Fig. 7D), cortical subpial layers (Fig. 7E) and deeper cortical layer VI (Fig. 7F) in both IFA and MOG + IFA LVLTα injected animals compared to LVGFP. There were no significant differences between GFAP numbers in IFA or MOG + IFA animals in any region examined (Fig. 7D–F).

The immunostaining results indicated activation of both microglia and astrocytes following LVLTα injection. Therefore, we further investigated the molecular phenotype of primary astrocytes and microglia following treatment with recombinant LTα, using data from several gene expression analysis papers examining changes in astrocytes and microglia during EAE to select genes known to change in models of multiple sclerosis (Supplementary Table 3).[54–56] Stimulation of astrocytes with recombinant LTα caused the upregulation of gene and protein expression for a number of proteins known to be secreted by secreted by astrocytes (SERPINA 3N, CXCL10), as well as several suggested to be linked to a disease like phenotype (GBPG2, C1RA, ICAM, VCAM, S100A10, PTGS2) (Fig. 7G). Transcript levels of receptors TNFR1 and TNFR2 were also strongly upregulated (Fig. 7H). Multiple chemokines and cytokines were upregulated in astrocytes, with the greatest increase seen for genes LTβ, IL-1β, CCL2 and CCL3 (Fig. 7H). Treatment of microglia with LTα led to upregulation of genes involved in several different pathways, including cytokine expression (Fig. 7I), phagocytotic markers (Fig. 7J), IFN signalling (Fig. 7K) and the complement pathway (Fig. 7L). The greatest upregulated gene in treated microglia was complement C1s with a 2308 ± 567-fold increase (Fig. 7L). To determine whether LTα activated microglia would be able to activate astrocytes, we treated astrocytes with LTα-conditioned medium from microglia (Fig. 7M). LTα stimulated microglial conditioned medium caused a significant upregulation of several astrocyte markers (GFAP, FGFR3, APOE, NOS2, GLT1 and S100β) associated with astrogliosis. Along with these there were large increases in transcription for pan-reactive genes (C4B, SERPINA3N, HLA-DQ, CD44, CXCL10) and disease associated phenotype markers (C3, C1RA, H2-T23). Interestingly, the largest gene change of all was a 9406-fold increase in S100A10 expression (Fig. 7M).

The subpial glial activation pattern in injected rats clearly suggested a direct activation of GM glia by the elevated presence of
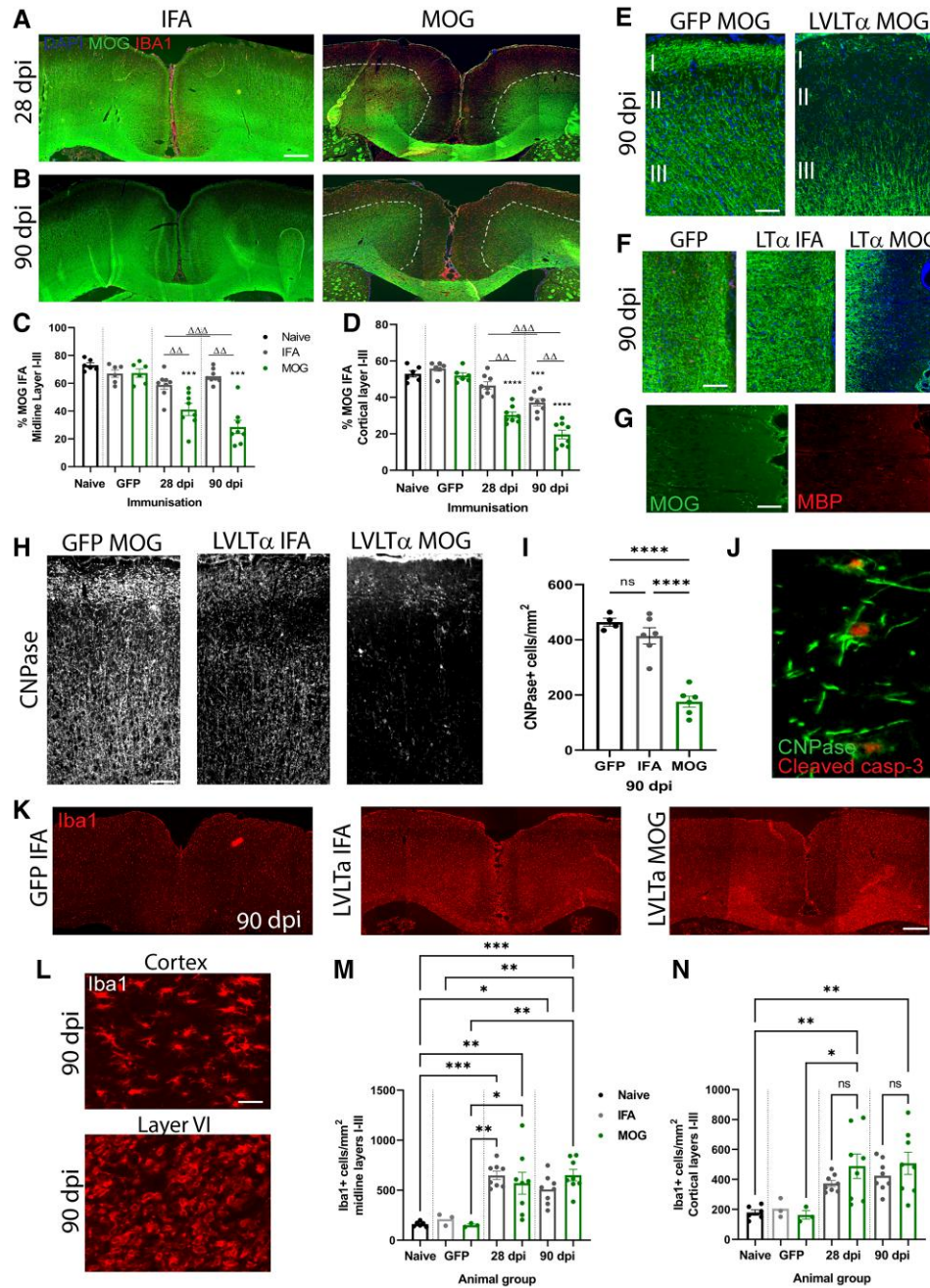
Figure 6 Demyelination and microglial activation after chronic overexpression of LTα. (**A** and **B**) Representative images of MOG staining in LVLTα in-jected animals immunized with IFA or MOG + IFA at 28 dpi (**A**) and 90 dpi (**B**). Demyelination was present in subpial areas in MOG + IFA-immunized rats at 28 and 90 days after LVLTα injection (delineated by dotted lines) but not in IFA-only immunized animals. (**C** and **D**) Quantification of subpial demye-lination in midline layers I–III (**C**) and cortical layers I–III (**D**) presented as the percentage area covered by MOG immunofluorescence (IF). Data is pre-sented as the mean ± SEM. Statistics: one-way analysis of variance with Tukey post-test. *** $P < 0.001$, **** $P < 0.0001$ LTa vector versus naïve; ${}^{ΔΔ}P < 0.01$, ${}^{ΔΔΔ}P < 0.001$ for MOG + IFA and IFA comparisons and between time points. Naïve and GFP groups $n = 6$, LVLTa groups $n = 8$. (**E** and **F**) Immunofluorescence for MOG at higher magnification shows no demyelination in eGFP vector-injected animals compared to MOG-immunized animals in layers I and II in the cortex (**E**) or midline (**F**) at 90 dpi. Demyelination in the midline was minimal in IFA LVLTα animals compared to MOG-immunized ones (**F**). (**G**) MBP immunostaining confirmed the lack of myelin shown by MOG immunostaining. (**H**) CNPase immunostaining in MOG + IFA-immunized animals in-jected with LVGFP compared to IFA-immunized and MOG + IFA-immunized LVLTα animals also confirmed the subpial demyelination in MOG-immunized animals. Scale bar = 100 μm. (**I**) Quantification of CNPase⁺ nuclei in layers I–III at 90 dpi confirmed loss of oligodendrocytes only in MOG + IFA-immunized LVLTα animals, when compared to IFA-immunized LVLTα animals and GFP vector control animals. Statistics: one-way analysis of variance with a Tukey *post hoc* test. **** $P < 0.0001$. (**J**) Co-localization of cleaved caspase-3 staining in CNPase+ cells. (**K**) IBA1 immunofluorescence revealed little microglial activation immediately surrounding the sagittal sulcus and SAS in MOG + IFA-immunized animals at 90 days post-LVGFP in-jection, whereas prominent microglial activation occurred throughout the corpus callosum and cortex following LVLTα injection in both IFA and MOG + IFA-immunized animals. (**L**) Ameboid IBA1+ cells were found in layer VI compared to ramified IBA1⁺ cells in the surface cortical layers. (**M**) Quantification of IBA1 cells/mm² showed significant increases in IBA1 cells/mm² at 28 and 90 dpi in midline layers. (**N**) In the surface cortical regions only MOG + IFA-immunized animals showed a significant increase in IBA1⁺ cell numbers. There was no significant difference between IFA or MOG-immunized animals. *$P < 0.05$, **$P < 0.01$, ***$P < 0.001$. Statistics one-way ANOVA with a Tukey *post hoc* test.
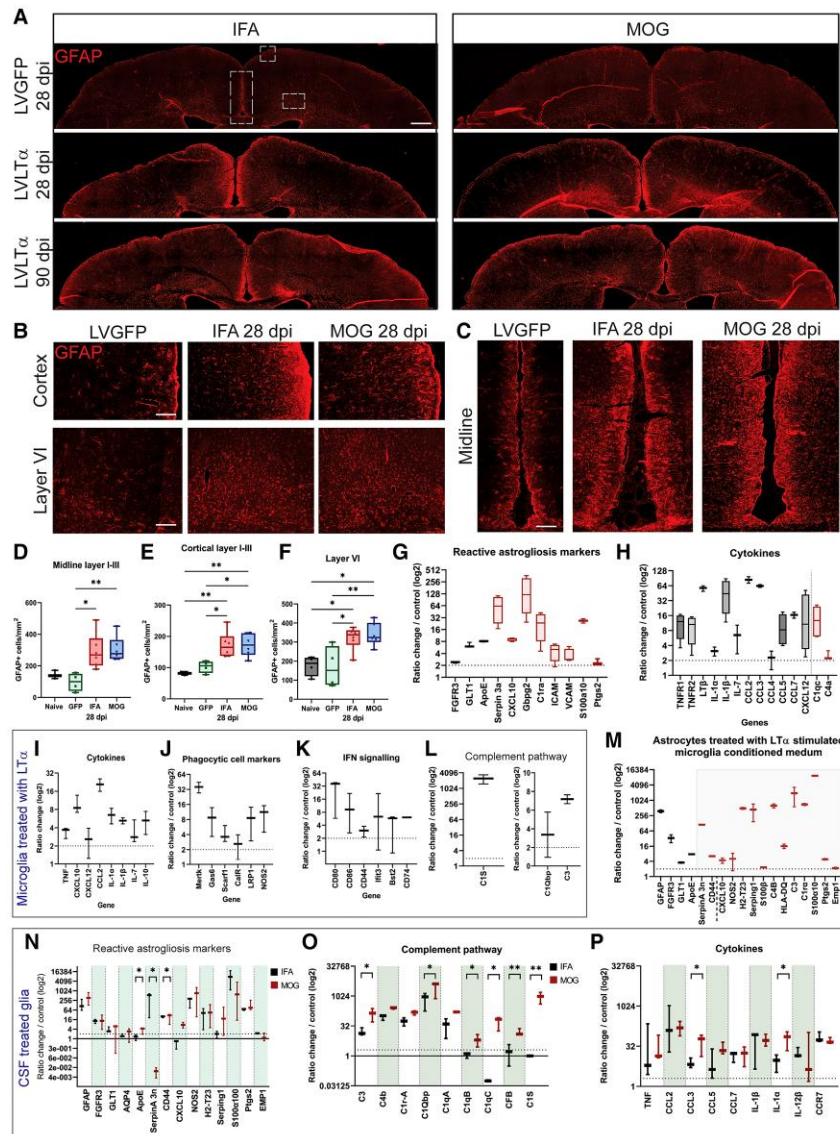
Figure 7 Astrocyte activation following chronic exposure to LTα *in vivo* and the response of astrocytes and microglia to LTα *in vitro*. (**A**) Representative images of GFAP immunostaining in rat cortex for LVGFP and LVLTα injected IFA and MOG + IFA-immunized animals. GFAP intensity is increased in both IFA and MOG + IFA LVLTα animals. Scale bar = 100 μm. Dashed squares on the first panel represent areas examined in **B**. (**B**) GFAP expression in cortical layers I–III and deeper cortical layer VI in LVGFP, and IFA and MOG + IFA LVLTα animals at 28 dpi. Scale bar = 30 μm. (**C**) GFAP expression in midline regions surrounding the SAS for LVLTα IFA and MOG + IFA-immunized animals and LVGFP animals at 28 dpi. (**D–F**) Quantification of GFAP+ cells per mm² in midline layer I–III regions (**D**), cortical layer I–III (**E**) and cortical layer VI (**F**) in naïve rats and after LVGFP or LVLTα injection in IFA and MOG + IFA-immunized animals. GFP animals showed no increase in GFAP numbers while LVLTα animals had significant increases in all regions examined. Graph presented is box-and-whisker plot with 10–90% range *P < 0.05, **P < 0.01. One-way ANOVA with a Tukey test. (**G**) Primary astrocyte cells were treated with 100 ng/ml LTα for 2 h before changing medium. Changes in gene expression were measured by RT–PCR after a further 24 h. (**G**) Shows gene expression changes for general astrocyte markers (GLT1, ApoE, FGFR3) and markers of reactive astrogliosis (Serpina3n, CXCL10Gbp2, C1ra, ICAM, VCAM, s100a10 and Ptgs2). (**H**) Shows changes in transcription for cytokines and TNFR1 and TNFR2 receptors. Ratio changes calculated for LTα treated over non-treated showed increased gene expression levels and all data shown on graph are significant at P < 0.05 with >2-fold ratio change. (**I–L**) Primary microglial cells were treated with 100 ng/ml LTα for 2 h before changing medium for fresh and harvesting cells 24 h later. Changes in gene expression measured by RT–PCR. Genes related to (**I**) cytokines, (**J**) phagocytic cell markers, (**K**) IFN signalling and (**L**) complement pathway that showed a significant fold change >2× based on a P-value <0.05 are shown in the graphs. Ratio changes calculated for LTα treated over non-treated. (**M**) Microglia LTα-conditioned medium was added to primary astrocytes for 24 h before examining changes in mRNA expression. Ratio change calculated as LTα-conditioned medium over naïve microglial medium. Microglial conditioned medium caused significant increases in mRNA for astrocytes markers (GFAP, ApoE, FGFR3, NOS2, S100b) and markers of reactive astrogliosis (Serpina3n, CXCL10, C4B, HLA-DQ, CD44, C3, C1ra, H2-T23, Serping1s100a10, EMP1 and Ptgs2). (**N–P**) Primary mixed glial cultures were treated with CSF from IFA-immunized or MOG + IFA-immunized animals injected with LVLTα or PBS as a control. Ratio changes were calculated for LVLTα CSF over PBS treated glia. All ratio changes shown on graph were significant compared to PBS treated, with a >2× ratio change based on a P < 0.05. (**N**) Changes in genes related to astrocyte activation. The only genes that were significantly different between IFA and MOG + IFA CSF were ApoE, Serpina3n and CD44 at *P < 0.01. (**O**) mRNA changes for components of the complement pathway showed several significant differences between IFA and MOG + IFA CSF-treated glia (C3, C1Qbp, C1qb, C1qc, CFB and C1S). *P < 0.05, **P < 0.01. (**P**) Measurement of cytokine gene changes after CSF treatment in glial cultures. There were significant differences between IFA and MOG + IFA CSF treatment for CCL3 and IL-1a. *P < 0.05. For all PCR graphs, error bars represent 95% confidence intervals. Statistics was performed using one-way ANOVA with a Tukey test on ΔCt data.

cytotoxic LTα within the CSF. However, it is likely that the presence of LTα also stimulated the release of other cytotoxins into the CSF. To investigate how glia might respond to CSF from LVLTα overexpressing rats we treated mixed glial cultures (astrocytes and microglia) with CSF from IFA or MOG + IFA-immunized animals injected with LVLTα. There was a similar upregulation of astrocyte-related genes as seen for treatment with recombinant LTα, with the exception of APOE, SERPINA3N and CXCL10, which were significantly higher in cells treated with CSF from MOG + IFA-immunized animals (Fig. 7N). Several components of the complement pathway were significantly higher in cells treated with CSF from MOG + IFA-immunized animals compared with cells treated with CSF from IFA-only immunized animals (C3, C1Qbp, C1qb, C1qc, CFB, C1s) (Fig. 7O). Examination of cytokine gene changes after CSF exposure showed very similar expression patterns between the MOG + IFA and the IFA-only immunized groups, with the exception of CCL3 (IFA 7.79 ± 1.94 versus MOG 58.81 ± 14.00) and IL-1a (IFA 9.34 ± 25 versus MOG 68.3 ± 29) that was higher in cells treated with CSF from MOG + IFA compared to IFA-only immunized animals (Fig. 7P).

Neuronal loss after persistent LTα overexpression

To determine whether chronic overexpression of LTα for 90 days would lead to cortical neurodegeneration, we counted neuronal numbers in multiple layers using NeuN immunostaining. In midline regions in close proximity to the meningeal aggregates there was a diffuse pattern of loss of neurons in layers I to III that extended the length of the sulcus (Fig. 8A). No neuronal loss was seen in GFP vector-injected animals, suggesting this loss was not the result of the surgical procedure. Quantification of midline NeuN+ cell numbers showed a similar loss in both IFA (34.0 ± 2.3%) and MOG (34.0 ± 3.3%) immunized animals compared to both naïve and GFP vector-injected animals (Fig. 8B). In the cortical parenchyma away from the midline, there were expansive regions throughout the motor and sensory cortices that demonstrated a marked decrease in NeuN+ cells, extending from the pial surface into the deeper cortical layers (Fig. 8C). Immunization with MOG also did not affect neuronal loss in the cortical layers away from the midline (Fig. 8D). In cortical layers II–III, there was a 40.0 ± 2.0% reduction in neuronal numbers in IFA and 33.0 ± 3.6% reduction in MOG + IFA-immunized animals compared to naïve. The cortical region with the most apparent loss of NeuN+ cells was the rostral cortex, where there were focal areas of loss that in some animals extended from the subpial surface down to layer IV (Fig. 8E). This loss was apparent in all animals injected with LTα vector, both IFA and MOG + IFA immunized. We also found a significant reduction in the density of layer V neurons in the midline (Fig. 8F and G). Examination of 200 kDa neurofilament protein immunostaining in midline regions showed a decrease in staining in midline regions accompanying the decrease in neuronal numbers (Fig. 8H). This reduction in cortical neuronal number was also accompanied by a decreased intensity of MAP2 staining in apical dendritic tufts and descending dendritic bundles that extend through to layers II/III (Fig. 8I). Neuronal loss was confirmed with immunostaining with antibodies against the HuC and HuD neuronal RNA binding proteins,[52] which showed a decreased density of neurons (Fig. 8J). To confirm that the neurons were dying via necroptosis, as shown previously for overexpression of TNF,[46,52] we used immunostaining for phosphorylated MLKL. MLKL is the final protein involved in the necroptosis pathway and once phosphorylated initiates cell death by forming oligomers which insert into the cell membrane to form a pore. pMLKL showed minimal expression in GFP animals, but in

IFA and MOG + IFA-immunized animals displayed a laminar pattern in layers II/III and IV (Fig. 8J, illustrated for IFA-only immunized animals). In these pMLKL+ HuC/D+ cells, the pMLKL was expressed within the cytoplasm and cell membrane (Fig. 8K).

Discussion

More extensive cortical demyelination and neurodegeneration in the multiple sclerosis brain, leading to an accelerated disease course (earlier age of clinical onset, more rapid disease progression and earlier age of death), has been shown to be associated with the presence of meningeal TLS formation[6,9,10,13] and an increasingly proinflammatory CSF milieu.[12,24] In this study, we provide experimental evidence that chronic production of LTα in the cortical SAS of the adult rat can induce lymphoid chemokine expression, the persistent presence of meningeal immune cell infiltrates with many features of tertiary lymphoid structures, and chronic pathology in the underlying cortical GM that includes subpial demyelination, microglial activation and accumulating neuronal loss. Such findings are remarkably similar to the pathological changes seen in the multiple sclerosis cerebral cortex in SPMS and provide some possible insights into the pathogenetic mechanisms involved.

Numerous previous studies have shown the presence of LTα and β in serum and CSF from progressive multiple sclerosis patients and their production by activated T and B cells.[33,35,57–59] In addition, the gene for LTα (LTA or TNFSF1) has been linked to multiple sclerosis susceptibility[60] and is suggested to play a role in the stimulation of relapses in RRMS.[32,61] However, its role in the link between compartmentalized inflammation and the pathogenesis of CNS damage has received little attention. In our study, LTα post-mortem CSF levels were highest in patients that displayed the greatest levels of meningeal inflammation and the presence of meningeal TLS. Increased levels of LTα gene expression in the isolated meninges strongly suggests a cellular source, most likely from activated memory B cells or CD4+ and CD8+ T cells.[58,62] B cells from untreated multiple sclerosis patients exhibit abnormal proinflammatory cytokine responses, in particular exaggerated production of LTα, when activated in the context of Th1 cytokine IFNγ or the presence of a TLR9 ligand.[63] Similarly, stimulation with a TLR9 agonist results in increased frequency of LTα producing B cells in patients with RRMS.[64] A significant increase in LTα secretion from anti-CD3-stimulated CD8+ T cells has also been reported in patients with SPMS compared to normal controls,[35] which is in agreement with the immunohistochemical localization of LTα in CD3+ T cells in the meningeal tissues in the current study. Thus, there is accumulating data suggesting a role for LTα in the continuing inflammation that is characteristic of progressive multiple sclerosis. It seems likely that in multiple sclerosis cases with prominent meningeal inflammation, LTα expressed by infiltrating cells within the cerebral sulci may induce a sufficient increase in the local LTα concentration to result in fibroblast differentiation into FDCs and induction of lymphoid chemokines, including CXCL13, CCL19 and CCL21, as is suggested to occur in rheumatoid arthritis synovium.[65–68]

Both acute and chronic elevation of LTα expression in the CSF were able to induce substantial immune cell infiltrates in the meninges that displayed a similar cellular composition to the meningeal inflammation reported in SPMS patients,[6,13,14] including those with short duration aggressive disease.[18] Although previous animal studies in both active and passive induction EAE models have described the presence of TLS at various stages of complexity
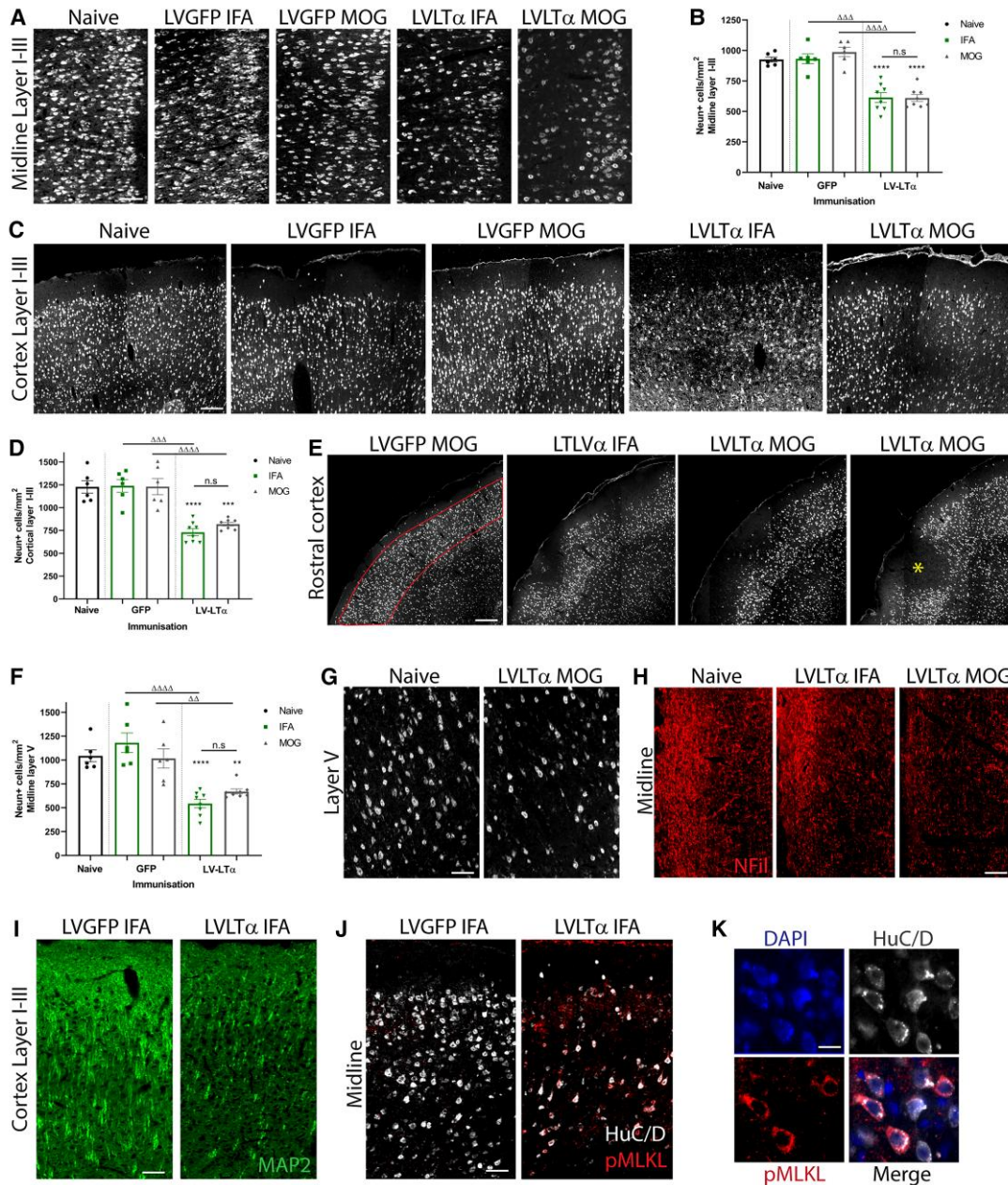
Figure 8 Neuronal loss in the cortical parenchyma after 90 days persistent LTα expression. (**A**) Representative images of NeuN immunofluorescence in midline layers I–III for naïve, LVGFP in IFA and MOG + IFA-immunized animals and LVLTα in IFA and MOG + IFA animals, showing a decreased neuronal density in LVLTα injected animals. Scale bar = 50 μm. (**B**) Quantification of NeuN$^+$ cells per mm^2 in midline layers I–III after LV injection. LVGFP animals had no decrease in NeuN+ cells while LVLTα animals had significant decreases in neuronal numbers both in IFA (613.8 cells/mm^2, $n = 8$) and MOG + IFA (609.6 cells/mm^2, $n = 8$) immunized animals compared to naïve (924.83 cells/mm^2, $n = 6$) and LVGFP groups. Data presented is mean ± SEM. ****$P < 0.0001$, ΔΔΔ$P < 0.001$, ΔΔΔΔ $P < 0.0001$. (**C**) Representative images of NeuN immunostaining in cortical layers I–III from motor cortex 90 days after cytokine or GFP vector injection. A decreased density of NeuN expressing neurons is seen in both IFA and MOG + IFA-immunized LVLTα injected, but not in LVGFP animals. Scale bar = 60 μm. (**D**) Graph showing mean number of NeuN$^+$ cells/mm^2 in cortical layers I–III in all animal groups. A significant loss of NeuN$^+$ cells is shown in both LVLTα injected IFA and MOG + IFA-immunized animals when compared to LVGFP and naïve animals. There was no significant difference between IFA and MOG + IFA-immunized LVLTα injected animals. ***$P < 0.001$, ****$P < 0.0001$ LVLTα versus naïve. ΔΔΔ $P < 0.001$, ΔΔΔΔ $P < 0.0001$ LVLTα IFA/MOG versus LVGFP. (**E**) Representative images of NeuN immunostaining in rostral cortical regions. Loss of NeuN immunostaining in LVLTα animals compared to naïve controls was most visibly apparent in rostral regions, with loss present in both IFA and MOG animals. One MOG animal had focal neuronal loss that extended from the pial surface down through to layer IV (star in final image). Scale bar = 100 μm. (**F**) Quantification of NeuN+ cells/mm^2 in midline layer V, showing similar losses to layers II–III. **$P < 0.01$, ****$P < 0.0001$ LVLTα versus naïve. ΔΔ $P < 0.01$, ΔΔΔΔ $P < 0.0001$ LVLTα IFA/MOG versus LVGFP. (**G**) NeuN+ staining in layer V of naïve and LVLTα MOG + IFA animals. In layer V there was a decrease in NeuN staining density, in particular for smaller size interneurons, rather than the larger pyramidal cells. (**H**) 200 kDa neurofilament protein immunofluorescence within the cortex in proximity to the midline showed a decreased density of staining in both IFA and MOG + IFA LVLTα animals compared to naïve controls. Scale bar = 50 μm. (**I**) Expression of MAP2 staining in IFA-immunized animals comparing LVGFP and LVLTα. (**J**) Reduced numbers of HuC/D$^+$ neurons in LVLTα animals compared to LVGFP. Costaining for HuC/D and pMLKL showed absence of pMLKL in GFP cortex and laminar expression of pMLKL in layers II/III and IV. (**K**) Costaining for HuC/D and pMLKL identified pMLKL-expressing necroptotic neurons where pMLKL was expressed in the cytoplasm and membrane compartments. Statistics: one-way ANOVA with a Tukey *post hoc* test.

in the meninges overlying the brainstem, cerebellum, spinal cord and in the ventricles,[39–43] none of these models exhibited the classical subpial cortical GM demyelinating and neurodegenerative pathology that is commonly seen in multiple sclerosis. By creating a focal model with persistent immune cell infiltration restricted to the meningeal space and extending down into the full depth of the sagittal sulcus as well as across the cortical surface, we have reproduced a number of features of the situation seen in multiple sclerosis, notably the presence of TLS neogenesis in deep sulci.[10,69] It is likely that the reduced CSF flow in the deep sulcus would allow a local increase in cytokine concentration that might not be reflected by global concentrations, although no experimental data is available on such CSF flow rates in the rat. In this regard it is also of interest that the EAE models in which TLS have been observed are characterized by a more chronic disease course,[39,41–43] which would allow inflammatory infiltrates to build up and be maintained. While TLS developed over a remarkably short time frame in the presence of acutely elevated LTα levels, it required persistent expression for them to be maintained. In keeping with this, persistent ectopic expression of LTα in peripheral organs in transgenic mice has been shown to lead to ectopic lymphoid neogenesis,[25,70] but similar experiments have not investigated its role in the CNS and related tissues. The described model allows the investigation of some of the consequences of targeted increased LTα expression and subsequent compartmentalized inflammation on tissue damage in a way that is closely relevant to multiple sclerosis itself.

Persistent LTα expression might be expected to create a permissive microenvironment for TLS formation by endowing meningeal stromal support cells 'immune competence' to secrete lymphocyte chemoattractants, such as CXCL13, CCL19 and CCL21, thus producing support networks for the interaction of B cells with T cells and local activation and further maturation. Our data suggests that LTα may act on a population of meningeal FDCs that then secrete CXCL13 and CCL19 in response to LTα stimulation, allowing the attraction and organization of B cells. A similar network of follicular dendritic cells expressing CXCL13 has also been reported in TLS in the multiple sclerosis brain.[9,13] It has been suggested that these FDCs are of stromal origin and could mature from ubiquitous local precursors such as PDGFRB+ pericytes in response to cytokines such as LTα[71] Discrete patterns of staining also suggest the presence in the meninges of a population of stromal FRCs that express podoplanin, CXCL12 and CCL21 and may help to form T-cell zones. A similar population of podoplanin+FRCs that secrete CCL21, as well as CXCL13 and BAFF, has been previously reported in the mouse SJL/J EAE model.[43] The precise composition of the meningeal cell infiltrate and the interaction with resident lymphoid inducing cells remains to be determined, both in this model and in multiple sclerosis itself. However, it is important to note that the development of the lymphoid-like tissues did not appear to require the presence of an antigen specific immune response as it occurred in both animals immunized with MOG plus IFA and IFA only.

Maintenance of the TLS structures once formed may also be driven by chemokine production by subpial astrocytes in close proximity to aggregates formed both in sulci and across the surface of the cortex. Treatment of astrocytes with LTα induced increased expression of the genes CCL3, CCL4, CCL5 and CCL7. These chemokines can act through CCR1 on B cells, T cells and dendritic cells, with several resulting functions involving chemotaxis, synthesis of inflammatory mediators and activation and recycling of leucocytes.[72] Levels of CCL3 and CCL4 in CSF show a positive correlation with severity of disease and disease duration in RRMS patients.[73] High local production of CXCL12 by pial astrocytes may also drive

the activation of FRCs in the meninges. Increased expression of IL-1α and IL-1β by both astrocytes and microglia after LTα exposure would further drive chemokine expression by infiltrating immune cells. This raises an interesting question of whether in the multiple sclerosis cortex subpial astrocytes activated by LTα from CSF and local factors from activated microglia would develop a phenotype sufficient to initiate meningeal aggregate formation.

The presence of many channels of variable diameter within the dense meningeal infiltrates at 28 and 90 days post-LTα vector injection included some that resembled the 'loose dilated' lymphatic vessels described previously in TLS in lung biopsies of idiopathic pulmonary arterial hypertension patients.[74] Smaller channels with thin walls expressing laminin, podoplanin and MadCam-1, with an absence of red blood cells, suggests the formation of HEVs.[75] Unfortunately, expression of LYVE-1 and PNAd could not be used to confirm the presence of true lymphatic vessels as all the human and mouse reactive antibodies failed to react with the rat proteins. While few studies examining TLS in EAE have reported the presence of HEVs in the meninges,[42,76,77] HEVs expressing MadCam-1 and PNAd have been reported in MP4-immunized mice[41] and in the PLP induced SJL/J EAE model.[40] Given that HEVs develop in response to LTα, it is possible their formation may only occur in the most mature TLOs or in cases with high LT levels.[78] The meningeal aggregates seen in the current model bear much resemblance to TLS that develop in the kidney and pancreas of rat insulin promoter-LT (RIP-LTα/β) mice with regard to cellular composition (T cells, B cells, plasma cells and antigen-presenting cells), delineated T- and B-cell areas and characteristic morphologic and antigenic (MAdCAM-1) features of HEVs.[25,70] This may indicate a very specific type of TLS that forms in the presence of LTα that may differ from those induced by other cytokines such as IL-17.[43] However, further studies are required to explain the detailed cellular and molecular mechanisms by which they form in the cerebral meninges. Although our results show that LTα can play a major role in the initial formation of such structures, other cytokines and chemokines that have been demonstrated to be present in the multiple sclerosis meninges and CSF undoubtedly contribute.[12]

Both acute and sustained LTα expression gave rise to subpial demyelinated lesions that extended from the pial surface down to cortical layer III/IV and demonstrated many similarities to key features of multiple sclerosis cortical lesion type III, in particular microglial activation, an absence of amoeboid macrophage-like cells and minimal lymphocytic infiltration. However, subpial demyelination required a pre-existing anti-MOG autoimmune response, as very minimal demyelination occurred in IFA-only immunized animals. The requirement for an anti-MOG response for demyelination to occur suggests that the microglial activation response may differ depending on previous immunization, such that activated microglia and astrocytes release different effector molecules in rmMOG-immunized compared to IFA rats, or that autoantibodies contribute to microglial-mediated demyelination in this model. Autoantibodies may also induce demyelination through activation of complement, and immunoglobulin and complement fragment deposition have been observed on myelin sheaths at the lesion edge in targeted EAE following subarachnoid and intracortical injection of TNF and IFNγ[21,50] and in human multiple sclerosis cortical GMLs,[79] suggesting that humoral immune mechanisms may contribute to demyelination in these models and in the current study. The difference in gene expression of complement pathway components between glia treated with CSF from IFA only and MOG + IFA-immunized animals supports the idea that

there is greater activation of the classical complement system in MOG-immunized animals. However, further detailed studies of the molecular changes in both microglia and astrocytes are required to dissect the mechanisms involved. It is likely that LTα is mainly involved in targeting the immune response to the surface of the cortex, rather than playing a direct cytotoxic role in oligodendrocyte cell death, as has been reported *in vitro*,[29] although this may contribute to the pathology. Following LTα exposure there was an upregulation of several genes (CD80, CD86, CD74, CXCL10) known to be expressed by M1 type microglia found in multiple sclerosis lesions,[80] They also expressed several markers associated with apoptotic cell uptake. It is possible that alterations of levels of these genes within microglia by LTα could influence how successfully they can clear myelin debris within lesions. The substantial areas of subpial demyelination that were observed in rmMOG-immunized rats at 28 and 90 days post-LVLTα, in contrast to the complete remyelination observed by 21 days after recombinant cytokine injection and in other targeted EAE models,[21,50,51] may represent chronic demyelination due to an eventual failure of remyelination, or overlapping cycles of demyelination and remyelination such that remyelination always appears incomplete. The pattern of demyelination suggests that complete failure ensues after longer time periods, although further studies are required to ascertain this.

Loss of neurons in the GM of the cerebral cortex of progressive multiple sclerosis brains, that is independent of demyelination, is a reproducible and widespread finding.[6,52,81–83] It is more substantial in cases with higher levels of meningeal inflammation and lymphoid tissue formation, when it occurs in a decreasing gradient from the pial surface towards the white matter.[6] We report here a similar pattern of neuronal loss in midline and surface cortical regions following chronic expression of LTα in the overlying meninges, which is independent of demyelination or previous MOG immunization. This neuronal loss is similar to that obtained previously with chronic meningeal expression of TNF + IFNγ[46] but in the case of LTα did not require the additional presence of IFNγ. Focal areas of neuronal loss were also found in the rostral cortex, including the somatosensory and secondary somatosensory cortex. Although the dense meningeal infiltrates did not spread this far across the cortex, it is possible that neurons in this region, which have been linked to walking and motor impairment in multiple sclerosis,[84–86] are more susceptible to the proinflammatory environment created by overexpression of LTα in the CSF. Further work is needed to understand why these neurons might be particularly vulnerable.

The finding that neuronal loss was similar between MOG + IFA and IFA-only immunized animals and independent of demyelination suggests that LTα can be directly or indirectly cytotoxic to neurons. The LTα homotrimer, unlike the TNF homotrimer, only exists as a soluble protein and can bind to TNFR1, TNFR2 and HVEM receptors.[87] Soluble TNF interaction with TNFR1 is known to predominantly stimulate cell death signalling, either apoptosis or necroptosis.[52,88,89] Although constitutive expression of TNFR1 is low in the healthy adult brain, it is significantly upregulated in multiple sclerosis and in the cortical GM is expressed predominantly on neurons.[45,52] In the presence of increased meningeal inflammation and in a proinflammatory environment, TNF/TNFR1 mediated signalling in the cortical GM is directed towards necroptotic neuronal death.[45,46,52] Therefore, it is likely that LTα could also directly stimulate neurodegeneration in the same way by binding to TNFR1, although more *in vivo* studies would be required to substantiate this. Like TNF, LTα can induce necroptosis with the

same potency *in vitro*, and like TNF, uses the RIPK1, RIPK3 and MLKL kinase cascade.[90] The expression of pMLKL in the membrane of neurons in subpial cortical and midline regions in the present study supports the idea that the main mechanism of neuronal loss in our model is through necroptosis, in agreement with our previous studies.[45,46,52] The finding that CSF LTα levels were highest in multiple sclerosis patients with the greatest cortical thinning also supports the hypothesis that LTα could be acting directly on neurons following diffusion through the damaged pial membrane.[6] LTα could also be acting indirectly by stimulating chronic microglial and astroglial activation and subsequent release of neurotoxic mediators,[8] which is supported by the extensive global microglial activation seen after chronic LTα expression in the current study. Increased levels of proinflammatory cytokines in the SAS have also been shown to give rise to increased endogenous parenchymal expression of TNF and IFNγ in the underlying cortical layers[46] and microglia in primary culture release glutamate in response to both LTα and TNF,[91] raising the possibility that neurodegeneration could occur indirectly via excitotoxicity. However, further experimental studies are required to determine the detailed mechanisms by which LTα could be inducing neurodegeneration in this rat model. Whether stimulation of the formation of TLS in the meninges in this model is due to a direct effect mediated by LTα/TNFR1 interaction or by LTα monomers becoming incorporated into the cell membrane as LTα$_2$β$_1$ or LTα$_1$β$_2$ heterotrimers that subsequently bind to the LTβR, also remains to be determined.

Both LTα alone and CSF from LVLTα rats induced activation of primary astrocytes that displayed a largely neurotoxic, proinflammatory phenotype based on gene changes. Astrocytes with a disease associated phenotype have been identified as having important roles in various proinflammatory pathways, including antigen presentation, complement pathway and interferon response pathway, all heavily implicated in multiple sclerosis. Liddelow *et al.*[92] showed that activated microglia could induce a neurotoxic phenotype in astrocytes by secreting IL-1α, TNF and C1q, all factors expressed by microglia after LTα exposure. After exposure to LTα-conditioned microglia medium, gene expression of C3 in astrocytes was very highly upregulated. C3$^+$ astrocytes are frequently found in the centre and expanding edge of actively demyelinating multiple sclerosis lesions, often in close proximity to activated microglia.[92] Disease associated astrocytes largely lose the ability to support neuronal survival, outgrowth and synaptogenesis and may make cortical neurons more vulnerable to cell death. In particular, C3 astrocyte expression is linked to a loss of synapses in demyelinating disease, that is independent of local demyelination and neuronal degeneration.[93] We propose that in our model LTα overexpression activates microglia, which then induces a neurotoxic phenotype in nearby astrocytes that become less supportive of neuronal survival and drive complement and antigen presentation pathways.

In conclusion, we have demonstrated that overexpression of LTα in the meningeal space in rats leads to chronic cortical pathology that replicates many of the neuropathological and molecular characteristics of multiple sclerosis, including meningeal inflammation with lymphoid tissue formation, microglial activation, demyelination and neuronal loss. We show that chronic LTα overexpression alone is sufficient to induce and maintain meningeal TLS. The detailed molecular mechanisms that cause some multiple sclerosis patients to develop meningeal TLS and ways to reduce the formation of these meningeal immune cell infiltrates can now be tested through the use of therapeutic interventions using this experimental model.

Acknowledgements

Funding

Competing interests

The authors report no competing interests.

Supplementary material

Supplementary material is available at *Brain* online.

References

1. Kutzelnigg A, Lucchinetti CF, Stadelmann C, *et al*. Cortical demyelination and diffuse white matter injury in multiple sclerosis. *Brain*. 2005;128:2705–2712.
2. Fisniku LK, Chard DT, Jackson JS, *et al*. Gray matter atrophy is related to long-term disability in multiple sclerosis. *Ann Neurol*. 2008;64:247–254.
3. Reynolds R, Roncaroli F, Nicholas R, Radotra B, Gveric D, Howell OW. The neuropathological basis of clinical progression in multiple sclerosis. *Acta Neuropathol*. 2011;122:155–170.
4. Calabrese M, Gajofatto A, Gobbin F, *et al*. Late-onset multiple sclerosis presenting with cognitive dysfunction and severe cortical/infratentorial atrophy. *Mult Scler*. 2015;21:580–589.
5. Harrison DM, Roy S, Oh J, *et al*. Association of cortical lesion burden on 7-T magnetic resonance imaging with cognition and disability in multiple sclerosis. *JAMA Neurol*. 2015;72:1004–1012.
6. Magliozzi R, Howell OW, Reeves C, *et al*. A gradient of neuronal loss and meningeal inflammation in multiple sclerosis. *Ann Neurol*. 2010;68:477–493.
7. Stadelmann C. Multiple sclerosis as a neurodegenerative disease: pathology, mechanisms and therapeutic implications. *Curr Opin Neurol*. 2011;24:224–229. doi:10.1097/WCO.0b013e328346056f
8. Calabrese M, Magliozzi R, Ciccarelli O, Geurts JJ, Reynolds R, Martin R. Exploring the origins of grey matter damage in multiple sclerosis. *Nat Rev Neurosci*. 2015;16:147–158.
9. Magliozzi R, Howell OW, Vora A, *et al*. Meningeal B-cell follicles in secondary progressive multiple sclerosis associate with early onset of disease and severe cortical pathology. *Brain*. 2007;130:1089–1104.
10. Howell OW, Reeves CA, Nicholas R, *et al*. Meningeal inflammation is widespread and linked to cortical pathology in multiple sclerosis. *Brain*. 2011;134:2755–2771.
11. Haider L, Zrzavy T, Hametner S, *et al*. The topography of demyelination and neurodegeneration in the multiple sclerosis brain. *Brain*. 2016;139:807–815.
12. Magliozzi R, Howell OW, Nicholas R, *et al*. Inflammatory intrathecal profiles and cortical damage in multiple sclerosis. *Ann Neurol*. 2018;83:739–755.
13. Serafini B, Rosicarelli B, Magliozzi R, Stigliano E, Aloisi F. Detection of ectopic B-cell follicles with germinal centers in the meninges of patients with secondary progressive multiple sclerosis. *Brain Pathol*. 2004;14:164–174.
14. Bell L, Lenhart A, Rosenwald A, Monoranu CM, Berberich-Siebelt F. Lymphoid aggregates in the CNS of progressive multiple sclerosis patients lack regulatory T cells. *Front Immunol*. 2019;10:3090.
15. Wang J, Jelcic I, Mühlenbruch L, *et al*. HLA-DR15 molecules jointly shape an autoreactive T cell repertoire in multiple sclerosis. *Cell*. 2020;183:1264–1281.e20. doi: 10.1016/j.cell.2020.09.054
16. Farina G, Magliozzi R, Pitteri M, *et al*. Increased cortical lesion load and intrathecal inflammation is associated with oligoclonal bands in multiple sclerosis patients: a combined CSF and MRI study. *J Neuroinflammation*. 2017;14:40.
17. Lucchinetti CF, Popescu BF, Bunyan RF, *et al*. Inflammatory cortical demyelination in early multiple sclerosis. *N Engl J Med*. 2011;365:2188–2197.
18. Bevan RJ, Evans R, Griffiths L, *et al*. Meningeal inflammation and cortical demyelination in acute multiple sclerosis. *Ann Neurol*. 2018;84:829–842.
19. Howell OW, Schulz-Trieglaff EK, Carassiti D, *et al*. Extensive grey matter pathology in the cerebellum in multiple sclerosis is linked to inflammation in the subarachnoid space. *Neuropathol Appl Neurobiol*. 2015;41:798–813.
20. Reali C, Magliozzi R, Roncaroli F, Nicholas R, Howell OW, Reynolds R. B cell rich meningeal inflammation associates with increased spinal cord pathology in multiple sclerosis. *Brain Pathol*. 2020;30:779–793.
21. Gardner C, Magliozzi R, Durrenberger PF, Howell OW, Rundle J, Reynolds R. Cortical grey matter demyelination can be induced by elevated pro-inflammatory cytokines in the subarachnoid space of MOG-immunized rats. *Brain*. 2013;136:3596–3608.
22. Dendrou CA, Fugger L, Friese MA. Immunopathology of multiple sclerosis. *Nat Rev Immunol*. 2015;15:545–558.
23. Pardini M, Brown WL, Magliozzi R, Reynolds R, Chard DT. Surface in pathology in multiple sclerosis: A new view on pathogenesis? *Brain*. 2021;144:1646–1654.
24. Magliozzi R, Scalfari A, Pisani AI, *et al*. The CSF profile linked to cortical damage predicts multiple sclerosis activity. *Ann Neurol*. 2020;88:562–573.
25. Kratz A, Campos-Neto A, Hanson MS, Ruddle NH. Chronic inflammation caused by lymphotoxin is lymphoid neogenesis. *J Exp Med*. 1996;183:1461–1472.
26. Gommerman JL, Browning JL. Lymphotoxin/light, lymphoid microenvironments and autoimmune disease. *Nat Rev Immunol*. 2003;3:642–655.
27. Gommerman JL, Giza K, Perper S, *et al*. A role for surface lymphotoxin in experimental autoimmune encephalomyelitis independent of LIGHT. *J Clin Invest*. 2003;112:755–767.
28. Selmaj K, Raine CS, Farooq M, Norton WT, Brosnan CF. Cytokine cytotoxicity against oligodendrocytes. Apoptosis induced by lymphotoxin. *J Immunol*. 1991;147:1522–1529.
29. Selmaj K, Raine CS, Cannella B, Brosnan CF. Identification of lymphotoxin and tumor necrosis factor in multiple sclerosis lesions. *J Clin Invest*. 1991;87:949–954.
30. Cannella B, Sizing ID, Benjamin CD, Browning JL, Raine CS. Antibodies to lymphotoxin alpha (LT alpha) and LT beta recognize different glial cell types in the central nervous system. *J Neuroimmunol*. 1997;78:172–179.

31. Raine CS, Bonetti B, Cannella B. Multiple sclerosis: expression of molecules of the tumor necrosis factor ligand and receptor families in relationship to the demyelinated plaque. *Rev Neurol (Paris)*. 1998;154:577–585.

32. Rieckmann P, Albrecht M, Kitze B, *et al*. Tumor necrosis factor-alpha messenger RNA expression in patients with relapsing-remitting multiple sclerosis is associated with disease activity. *Ann Neurol*. 1995;37:82–88.

33. Matusevicius D, Navikas V, Soderstrom M, *et al*. Multiple sclerosis: The proinflammatory cytokines lymphotoxin-alpha and tumour necrosis factor-alpha are upregulated in cerebrospinal fluid mononuclear cells. *J Neuroimmunol*. 1996;66:115–123.

34. Christensen J R, Bornsen L, Ratzer R, *et al*. Systemic inflammation in progressive multiple sclerosis involves follicular T-helper, Th17- and activated B-cells and correlates with progression. *PLoS ONE*. 2013;8:e57820.

35. Buckle GJ, Hollsberg P, Hafler DA. Activated CD8+ T cells in secondary progressive MS secrete lymphotoxin. *Neurology*. 2003;60:702–705.

36. De Togni P, Goellner J, Ruddle NH, *et al*. Abnormal development of peripheral lymphoid organs in mice deficient in lymphotoxin. *Science*. 1994;264:703–707.

37. Suen WE, Bergman CM, Hjelmstrom P, Ruddle NH. A critical role for lymphotoxin in experimental allergic encephalomyelitis. *J Exp Med*. 1997;186:1233–1240.

38. Hirose T, Fukuma Y, Takeshita A, Nishida K. The role of lymphotoxin-alpha in rheumatoid arthritis. *Inflamm Res*. 2018;67:495–501.

39. Magliozzi R, Columba-Cabezas S, Serafini B, Aloisi F. Intracerebral expression of CXCL13 and BAFF is accompanied by formation of lymphoid follicle-like structures in the meninges of mice with relapsing experimental autoimmune encephalomyelitis. *J Neuroimmunol*. 2004;148:11–23.

40. Bhargava P, Kim S, Reyes AA, *et al*. Imaging meningeal inflammation in CNS autoimmunity identifies a therapeutic role for BTK inhibition. *Brain*. 2021;144:1396–1408.

41. Kuerten S, Schickel A, Kerkloh C, *et al*. Tertiary lymphoid organ development coincides with determinant spreading of the myelin-specific T cell response. *Acta Neuropathol*. 2012;124:861–873.

42. Peters A, Pitcher LA, Sullivan JM, *et al*. Th17 cells induce ectopic lymphoid follicles in central nervous system tissue inflammation. *Immunity*. 2011;35:986–996.

43. Pikor NB, Astarita JL, Summers-Deluca L, *et al*. Integration of Th17- and lymphotoxin-derived signals initiates meningeal-resident stromal cell remodeling to propagate neuroinflammation. *Immunity*. 2015;43:1160–1173.

44. Mitsdoerffer M, Peters A. Tertiary lymphoid organs in central nervous system autoimmunity. *Front Immunol*. 2016;7:451.

45. Magliozzi R, Howell OW, Durrenberger P, *et al*. Meningeal inflammation changes the balance of TNF signalling in cortical grey matter in multiple sclerosis. *J Neuroinflammation*. 2019;16:259.

46. James RE, Schalks R, Browne E, *et al*. Persistent elevation of intrathecal pro-inflammatory cytokines leads to multiple sclerosis-like cortical demyelination and neurodegeneration. *Acta Neuropathol Commun*. 2020;8:66.

47. Durrenberger PF, Fernando FS, Magliozzi R, *et al*. Selection of novel reference genes for use in the human central nervous system: A BrainNet Europe study. *Acta Neuropathol*. 2012;124:893–903.

48. Papadopoulos D, Pham-Dinh D, Reynolds R. Axon loss is responsible for chronic neurological deficit following inflammatory demyelination in the rat. *Exp Neurol*. 2006;197:373–385.

49. Kerschensteiner M, Stadelmann C, Buddeberg BS, *et al*. Targeting experimental autoimmune encephalomyelitis lesions to a predetermined axonal tract system allows for refined behavioral testing in an animal model of multiple sclerosis. *Am J Pathol*. 2004;164:1455–1469.

50. Merkler D, Ernsting T, Kerschensteiner M, Bruck W, Stadelmann C. A new focal EAE model of cortical demyelination: Multiple sclerosis-like lesions with rapid resolution of inflammation and extensive remyelination. *Brain*. 2006;129:1972–1983.

51. Rodriguez EG, Wegner C, Kreutzfeldt M, *et al*. Oligodendroglia in cortical multiple sclerosis lesions decrease with disease progression, but regenerate after repeated experimental demyelination. *Acta Neuropathol*. 2014;128:231–246.

52. Picon C, Jayaraman A, James R, *et al*. Neuron–specific activation of necroptosis signaling in multiple sclerosis cortical grey matter. *Acta Neuropathol*. 2021;141:585–604.

53. Benezech C, White A, Mader E, *et al*. Ontogeny of stromal organizer cells during lymph node development. *J Immunol*. 2010;184:4521–4530.

54. Borggrewe MC, Grit ID, Vainchtein N, *et al*. Regionally diverse astrocyte subtypes and their heterogeneous response to EAE. *Glia*. 2021;69:1140–1154.

55. Itoh N, Itoh Y, Tassoni A, *et al*. Cell-specific and region-specific transcriptomics in the multiple sclerosis model: Focus on astrocytes. *Proc Natl Acad Sci U S A*. 2018;115:E302–E309.

56. Moreno-Garcia A, Bernal-Chico A, Colomer T, Rodrigues-Antiguedad A, Matute C, Mato S. Gene expression analysis of astrocyte and microglia endocannabinoid signalling during autoimmune demyelination. *Biomolecules*. 2020;10:1228.

57. Corcione A, Casazza S, Ferretti E, *et al*. Recapitulation of B cell differentiation in the central nervous system of patients with multiple sclerosis. *Proc Natl Acad Sci U S A*. 2004;101:11064–11069.

58. Duddy M, Niino M, Adatia F, *et al*. Distinct effector cytokine profiles of memory and naive human B cell subsets and implication in multiple sclerosis. *J Immunol*. 2007;178:6092–6099.

59. Christensen AD, Skov S, Haase C. Local and systemic effects of co-stimulatory blockade using cytotoxic T lymphocyte antigen-4-immunoglobulin in dinitrofluorobenzene- and oxazolone-induced contact hypersensitivity in mice. *Clin Exp Immunol*. 2013;171:220–230.

60. Fernandes Filho JA, Vedeler CA, Myhr KM, Nyland H, Pandey JP. TNF-alpha and -beta gene polymorphisms in multiple sclerosis: A highly significant role for determinants in the first intron of the TNF-beta gene. *Autoimmunity*. 2002;35:377–380.

61. Navikas V, He B, Link J, *et al*. Augmented expression of tumour necrosis factor-alpha and lymphotoxin in mononuclear cells in multiple sclerosis and optic neuritis. *Brain*. 1996;119:213–223.

62. Yang K, Liang Y, Sun Z, *et al*. T cell-derived lymphotoxin limits Th1 response during HSV-1 infection. *Sci Rep*. 2018;8:17727.

63. Bar-Or A, Fawaz L, Fan B, *et al*. Abnormal B-cell cytokine responses a trigger of T-cell-mediated disease in MS? *Ann Neurol*. 2010;67:452–461.

64. McWilliam O, Sellebjerg F, Marquart HV, von Essen MR. B cells from patients with multiple sclerosis have a pathogenic phenotype and increased LTalpha and TGFbeta1 response. *J Neuroimmunol*. 2018;324:157–164.

65. Lindhout E, van Eijk M, van Pel M, Lindeman J, Dinant HJ, de Groot C. Fibroblast-like synoviocytes from rheumatoid arthritis patients have intrinsic properties of follicular dendritic cells. *J Immunol*. 1999;162:5949–5956.

66. van Nierop K, de Groot C. Human follicular dendritic cells: Function, origin and development. *Semin Immunol*. 2002;14:251–257.

67. GeurtsvanKessel CH, Willart MA, Bergen IM, *et al*. Dendritic cells are crucial for maintenance of tertiary lymphoid structures in the lung of influenza virus-infected mice. *J Exp Med*. 2009;206:2339–2349.

68. Kain MJ, Owens BM. Stromal cell regulation of homeostatic and inflammatory lymphoid organogenesis. *Immunology*. 2013;140:12–21.

69. Griffiths L, Reynolds R, Evans R, *et al.* Substantial subpial cortical demyelination in progressive multiple sclerosis: Have we underestimated the extent of cortical pathology? *Neuroimmunol Neuroinflammation.* 2020;7:51–67.

70. Drayton DL, Ying X, Lee J, Lesslauer W, Ruddle NH. Ectopic LT alpha beta directs lymphoid organ neogenesis with concomitant expression of peripheral node addressin and a HEV-restricted sulfotransferase. *J Exp Med.* 2003;197:1153–1163.

71. Krautler NJ, Kana V, Kranich J, *et al.* Follicular dendritic cells emerge from ubiquitous perivascular precursors. *Cell.* 2012;150:194–206.

72. Benet Z, Marthi M, Ke F, *et al.* CCL3 Promotes germinal B cells sampling by follicular regulatory T cells in murine lymph nodes. *Front Immunol.* 2018;9:2044.

73. Soleimani M, Soleymani A, Seyyedirad N. Elevated CSF concentration of CCL3 and CCL4 in relapsing remitting multiple sclerosis patients. *J Immunoassay Immunochem.* 2019;40:378–385.

74. Perros F, Dorfmuller P, Montani D, *et al.* Pulmonary lymphoid neogenesis in idiopathic pulmonary arterial hypertension. *Am J Respir Crit Care Med.* 2012;185:311–321.

75. Herzog BH, Fu J, Wilson SJ, *et al.* Podoplanin maintains high endothelial venule integrity by interacting with platelet CLEC-2. *Nature.* 2013;502:105–109

76. Dang AK, Tesfagiorgis Y, Jain RW, Craig HC, Kerfoot SM. Meningeal infiltration of the spinal cord by non-classically activated B cells is associated with chronic disease course in a spontaneous B cell-dependent model of CNS autoimmune disease. *Front Immunol.* 2015;6:470. doi: 10.3389/fimmu.2015.00470

77. Cohen M, Giladi A, Raposo C, *et al.* Meningeal lymphoid structures are activated under acute and chronic spinal cord pathologies. *Life Sci Alliance.* 2020;4:e202000907.

78. Browning JL, Allaire N, Ngam-Ek A, *et al.* Lymphotoxin–beta receptor signaling is required for the homeostatic control of HEV differentiation and function. *Immunity.* 2005;23:539–550.

79. Watkins LM, Neal JW, Loveless S, *et al.* Complement is activated in progressive multiple sclerosis cortical grey matter lesions. *J Neuroinflammation.* 2016;13:161.

80. Peferoen L, Daphne M, Vogel D, *et al.* Activation status of human microglia is dependent on lesion formation stage and remyelination in multiple sclerosis. *J Neuropathol Expo Neurol.* 2015;74:48–63.

81. Yates RL, Esiri MM, Palace J, Jacobs B, Perera R, DeLuca GC. Fibrin(ogen) and neurodegeneration in the progressive multiple sclerosis cortex. *Ann Neurol.* 2017;82:259–270.

82. Carassiti D, Altmann DR, Petrova N, Pakkenberg B, Scaravilli F, Schmierer K. Neuronal loss, demyelination and volume change in the multiple sclerosis neocortex. *Neuropathol Appl Neurobiol.* 2018;44:377–390.

83. Trapp BD, Vignos M, Dudman J, *et al.* Cortical neuronal densities and cerebral white matter demyelination in multiple sclerosis: A retrospective study. *Lancet Neurol.* 2018;17:870–884.

84. Arpin DJ, Gehringer JE, Wilson TW, Kurz MJ. A reduced somatosensory gating response in individuals with multiple sclerosis is related to walking impairment. *J Neurophysiol.* 2017;118:2052–2058.

85. Arpin DJ, Heinrichs-Graham E, Gehringer JE, Zabad R, Wilson TW, Kurz MJ. Altered sensorimotor cortical oscillations in individuals with multiple sclerosis suggests a faulty internal model. *Hum Brain Mapp.* 2017;38:4009–4018.

86. Strik M, Chard DT, Dekker I, *et al.* Increased functional sensorimotor network efficiency relates to disability in multiple sclerosis. *Mult Scler.* 2021;27:1364–1373.

87. Medvedev AE, Espevik T, Ranges G, Sundan A. Distinct roles of the two tumor necrosis factor (TNF) receptors in modulating TNF and lymphotoxin alpha effects. *J Biol Chem.* 1996;271:9778–9784.

88. Ofengeim D, Yuan J. Regulation of RIP1 kinase signalling at the crossroads of inflammation and cell death. *Nat Rev Mol Cell Biol.* 2013;14:727–736.

89. Probert L. TNF And its receptors in the CNS: The essential, the desirable and the deleterious effects. *Neuroscience.* 2015;302:2–22.

90. Etemadi N, Holien JK, Chau D, *et al.* Lymphotoxin alpha induces apoptosis, necroptosis and inflammatory signals with the same potency as tumour necrosis factor. *FEBS J.* 2013;280:5283–5297.

91. Gallego-Delgado P, James R, Browne E, *et al.* Neuroinflammation in the normal-appearing white matter (NAWM) of the multiple sclerosis brain causes abnormalities at the nodes of Ranvier. *PLoS Biol.* 2020;18:e3001008.

92. Liddelow SA, Guttenplan KA, Clarke LE, *et al.* Neurotoxic reactive astrocytes are induced by activated microglia. *Nature.* 2017;541:481–487.

93. Werneburg S, Jung S, Kunjamma RB, *et al.* Targeted complement inhibition at synapses prevents microglial synaptic engulfment and synapse loss in demyelinating disease. *Immunity.* 2020;52:167–182.e7.